Spatial and temporal organization of the exocyst complex

Bachelor thesis in Biochemistry

Fabian Henneberg

geboren am

25.04.1990

in

München

Bachelorarbeit beim Prüfungsausschuss eingereicht am 17.09.2012

Erklärung

Ich versichere, dass ich die vorgelegte Bachelorarbeit am

Max Planck Institute of Biochemistry in Arbeitsgruppe Cellular Dynamics and Cell patterning, geleitet von Herrn Dr. Roland Wedlich-Söldner

unter der Anregung und Anleitung von

Dr. Roland Wedlich-Söldner und Dr. Felix Spira

selbständig durchgeführt und keine anderen als die angegebenen Hilfsmittel und Quellen benützt habe.

München, ...

.....

Unterschrift

Erstgutachter: .....

Zweitgutachter: .....

List of abbreviations

a.u.	arbitrary unit
bp	base pairs
C°	Celsius
ConA	Concanavalin A
DNA	deoyribonucleic acid
EM	electron microscopy
FRAP	Fluorescence Recovery after Photobleaching
GAP	GTPase activating protein
GEF	guanine nucleotide exchange factor
GFP	green fluorescence protein
GTP	guanosine triphosphate
g	gram
h	hour
His	Histidine
hphNTI	hygromycin
L	liter
m	meter
M	molar
min	minute
natNT2	Nourseothricin
OD	optical density
PCR	polymerase chain reaction
$PI(4,5)P_2$	phosphatidylinositol 4, 5-biphosphate
RFP	red fluorescence protein
RNA	ribonucleic acid
rpm	revolutions per minute
s	distance
sec	second
SNARE	soluble N-etylmaleimide-sensitive-factor attachment receptors
t	time
TIR	total internal reflection
UV	Ultraviolet
V	Volt
Vol	Volume

Summary

Exocytosis is divided into three steps: tethering, docking and fusion. Tethering is mediated by the exocyst complex, the first and essential step, which regulates when and where exocytosis takes place. The exocyst complex is composed of eight subunits (Sec3, Sec5, Sec6, Sec8, Sec10, Sec15, Exo70, and Exo84). Interactions between the subunits themselves are well studied and some interactions between subunits and other regulatory proteins, like monomeric GTPases, are known. Nevertheless the exact regulatory mechanism and function still remains unclear.

TIRF microscopy was used to investigate the spatio and temporal organization. The quantification of the subunits was done by using the TIRF microscope in an epifluorescence mode. Single color strains in which one subunit was tagged with GFP and double color strains, in which one subunit was tagged with GFP and another with the RFP mKate2, revealed the tagged subunits of the complex arrive together at the plasma membrane. The quantification of the subunits was done by comparison of the intensities of the GFP-tagged subunits with the intensity of the endogenous marker Cse4, a CENH3 histone variant, which was tagged with GFP. With data of the quantification experiment we concluded that about 26 exocyst complexes are bound to one vesicle. Each of these complexes is composed of subunits with a stoichiometry of 1:1.

Zusammenfassung

Der Exocytose Prozess besteht aus drei Schritten: Tethering, Docking und Fusion. Tethering, der erste und essentielle Schritt, welcher den Zeitpunkt und Ort der Exocystose festlegt, wird durch den Exocyst Komplex vermittelt. Der Komplex besteht aus acht Untereinheiten (Sec3, Sec5, Sec6, Sec8, Sec10, Sec15, Exo70, Exo84). Interaktionen zwischen den einzelnen Untereinheiten und Interaktionen zwischen Untereinheiten und regulatorischen Proteinen, wie den monomeric GTPasen, sind bisher untersucht worden. Dennoch sind die genauen regulatorischen Mechanismen und die Aufgaben des Komplexes noch nicht gut verstanden.

Die zeitliche und räumliche Organisation des Exocyst Komplexes wurde mit Hilfe des TIRF Mikroskop untersucht. Außerdem wurden eine Quantifizierung der Untereinheiten des Komplexes mit dem TIRF Mikroskop im Epi Fluoreszenz Modus durchgeführt. Zur Untersuchung der Komplex Organisation wurden Einzelfarben Stämme, in welchen eine Untereinheit mit GFP getaggt wurde, und Doppelfarben Stämme, in welchen eine Untereinheit mit GFP und eine andere Untereinheit mit mKate2 getaggt wurde, benutzt. Den Experimenten zufolge kommen die getaggten Untereinheiten zusammen an der Plasma Membran an. Durch einen Vergleich der Intensitäten der mit GFP getaggten Untereinheiten mit dem endogenen Marker Cse4, eine CENH3 Histonen Variante, der ebenfalls mit GFP getaggt wurde, wurden die Untereinheiten quantifiziert. Demnach befinden sich an einem Vesikel 26 Exocyst Komplexe. Diese Komplexe bestehen aus Untereinheiten, die eine Stöchiometrie von 1:1 aufweisen.

Table of contents

1. Introduction

1.1. The exocyst complex

The process to incorporate proteins and lipids into the plasma membrane or the release of molecules to the extracellular space by fusion of cargo filled vesicles with the plasma membrane is called exocytosis or secretion [1, 2]. Exocytosis is an important biological process in the cell which regulates cell growth, morphogenesis, cell migration and cell signaling [3].

Exocytotic vesicles generated at the tans Golgi network or endosomal compartments are delivered along the cytoskeleton to the plasma membrane [2, 4]. Exocytosis is divided into three steps: Tethering, docking and fusion [2]. Tethering is mediated by the exocyst complex. Three different proteins called soluble N-etylmaleimide-sensitive-factor attachment receptors (SNAREs) are required for docking and fusion. The v-SNARE Snc1 protein is localized on the exocytic vesicles, whereas the t-SNARE Sso1 is localized at the plasma membrane [5]. Both SNAREs connect to the membrane via a C-terminal transmembrane anchor [5]. A second t-SNARE Sec9 is localized at the plasma membrane but does not have a transmembrane anchor and is needed to form v-SNARE-t-SNARE complex of the proteins Sso1 and Snc1 for vesicle fusion [5].

The exocyst complex is an octameric complex composed of Sec3, Sec5, Sec6, Sec8, Sec10, Sec15, Exo70 and Exo84. The exocyst complex is highly conserved in all eukaryotic systems [6]. All subunits are essential except Sec3 which is redundant [7]. With yeast two-hybrid assays and binding experiments using either *in vitro*-translated or purified recombinant proteins, interactions between the subunits were revealed [4]. Most of the exocyst subunits can interact with multiple exocyst subunits of the complex suggesting conserved binding sides [8].

The exocyst complex is a member of the Complex Associated with Tethering Containing Helical Rods (CATCHR) family which have low sequence identity but conserved helical bundle structures [1]. The rod-like motif is a common feature of all subunits, although the sequences of the subunits are little conserved [4]. Two or more consecutively helical bundles consisting of three to five α-helices linked by flexible linkers form the rod-like motif [8]. The 'Y-shaped' structure of the exocyst complex revealed by EM pictures suggest the subunits packed in a side- to-side fashion along the rod-like structure [4].

Additional domains, unique hydrophobic and electrostatic patterns of individual subunits lead to own characteristics in spite of the common rod-like structure [1]. Sec3 contains a polybasic region at the N-terminal domain which interacts with phosphatidylinositol 4, 5-biphosphate ($PI(4,5)P_2$) at the

inner leaflet of the plasma membrane. Also Exo70 has basic residues which can interact with $PI(4,5)P_2$ [9]. It is likely these proteins tether the exocyst complex to the target membrane.

Exocyst tethering of the vesicles controls the spatial and temporal activity of exocytosis. The complex is highly regulated by several small monomeric GTPases. Monomeric GTPases are key players relaying signals. They are regulated by gunanine nucleotide exchange factors (GEFs) and GTPase-activating proteins (GAPs). GEFs are promoting the release of bound GDP to bind GTP to activate monomeric GTPases. Activated monomeric GTPases can relay signals of different molecules. In contrast the GAPs causes a higher hydrolysation rate driving the protein into an off state to stop relaying of the signals [10]. Rab-GTPases and Rho-GTPases are members of the Ras superfamily of monomeric GTPases. Rab-GTPases are known to play a central part in membrane trafficking. The GTP-bound form of the Rab-GTPase Sec4 bound to a vesicle directly interacts with Sec15 to regulate the assembly of the exocyst complex [11]. Rho-GTPases regulates a broad spectrum, the actin and microtubule cytoskeleton, cell shape, polarity, motility, adhesion, cell-cycle progression, gene transcription, and membrane transport[1]. Cdc42, a Rho-GTPases, which regulates establishing cell polarity and controlling polarized exocytosis, and the Rho-GTPases Rho1 interact with the N-terminus of Sec3 [2]. The exocyst subunit Exo70 is also a downstream effector of Cdc42 and of the monomeric Rho-GTPase Rho3 which regulates the exocytosis [2].

After the exocyst complex is tethered to the target membrane, fusion is mediated by SNARE proteins. Interactions of exocyst subunits with SNARE proteins were identified. The t-SNARE Sec9 and the other t-SNARE Sso1 can interact with Sec6 [3]. The SNARE regulatory protein Sec1 was indentified to interact with Sec6 [12]. The exocyst subunit Exo84 associates with Sro7 which is a member of the giant larvae tumor suppressor family[13]. Sro7 interacts and activates the t-SNARE Sec9 and is an downstream effector of Sec4 [13]. All in all the exocyst serves as a hub of regulatory proteins to control the exocytosis.

The assembly and disassembly of the complex is still unclear. FRAP experiments suggests that six of the eight subunits are bound to the vesicle during the delivery and transported along the cytoskeleton to the plasma membrane [14]. The remaining subunits Exo70 and Sec3 are localizing independently of this mechanisms but Exo70 can also be delivered using the cytoskeleton [14]. Exo70 and Sec3 are proposed to be landmarks waiting for subunits of the exocyst complex [1]. The first aim of the bachelor thesis was to clarify the assembly process. Single and double color tagged strain were measured with the TIRF microscope to detect the temporal and spatial organization of the exocyst complex.

An open question in the field is the stoichioemtrie of individual subunits of the exocyst complex. To study the mechanism of the exocyst assembly, fusion and cargo delivery in detail, the stoichiometry of individual subunits has to be known. This question was the starting point for the second aim of the bachelor thesis. The quantification of the exocyst complex was conducted by comparison of intensities of GFP tagged subunits with intensities of GFP tagged Cse4 proteins, which is a CENH3 histone variant in budding yeast.

The budding yeast CenH3 histone variant Cse4 is an important part of the centromeric nucleosomes. During replication of budding yeast it is the point where the kinetochores attach to segregate the chromosomes [15]. Cse4 can be used as a reference marker for protein counting because the kinetochores forms a near-diffraction limited spot during metaphase to late anaphase and because biochemical analysis suggested that every CEN DNA contains one copy of Cse4 [16]. The fluorescence spot was proposed to contain 32 molecules [17]. Recent papers revealed that every CEN DNA contains 5- 8 copies of Cse4 [16],[15]. Subsequently, the fluorescence spot of Cse4 correspond to 80 – 128 molecules.

1.2. Total internal reflection fluorescence microscope (TIRFM)

All measurements in this bachelor thesis were conducted using TIRF microscope. The big advantage of this type of microscope is selective excitation of fluorophores near a surface within a range of ≤ 100 nm by evanescent wave [18]. This technique selectively excites molecules close the coverslip and minimizes out of focus light. Thus images with very low background and almost no out-of-focus fluorescence are obtained [19].

Total internal reflection (TIR) occurs when a laser beam propagates through media from a higher refractive index to a lower refractive index and penetrates the interface under a certain incident angle which is measured from the normal. This incident angle can be calculated with Snell's law.

$$n_1 \sin\theta_i = n_2 \sin\theta_t$$

n_1= $high\ refractive\ index\ (e.g. solid)$

$n_2 = low\ refractive\ index\ (e.g. liquid)$

$\theta_i = incident\ angle$

$\theta_t = transmitted\ angle$

The critical angle is when $\theta_t = 0$. Therefore the critical angle can be calculated with the following formula.

$$\theta_c = \theta_i = \sin^{-1}\left(\frac{n_2}{n_1}\right)$$

$$\theta_c = critical\ angle$$

TIR do not occur if the ratio between n_1/n_2 is above 1 hence no $\sin^{-1}$ value exists for this ratio. In case the incident angle is smaller than the critical angle the laser beam would be refracted at the interface. If the incident angle is greater than the critical angle the laser beam is total reflected. As a side effect of TIR some of the incident energy generates an evanescent wave propagating parallel through the interface. The evanescent wave excites only fluorophores located 100 nm located close to the interface, because it decays exponential with distance z perpendicular to the interface [19].

2. Material and Methods

2.1.Material

2.1.1. Chemicals

Table 1: Chemicals used in the experiments

Chemicals	Supplier
Sodium hydroxide pellets	Sigma- Aldrich
Agarose powder	Invitrogen
Ethidiumbromide 1%	Carl Roth
SYBR® Green	Invitrogen
DNA 6x loading dye	Custom made
Concanavalin A 2mg/mL	Custom made
D(+)- Glucose anhydrous	Sigma- Aldrich
Absolute ethanol	Sigma- Aldrich
ddH_2O	Custom made
Immersion oil	Zeiss
Solmon sperm DNA	Invitrogen
DMSO	Sigma- Aldrich
Triton X-100	Carl Roth
SDS	Carl Roth
Sodiumchloride	Sigma- Aldrich
TrisHCl	CalBiochem
$Na_2EDTA{\cdot}2H_2O$	Merck
Phenol/ Chloroform	Carl Roth
dNTPs	New England BioLabs
Glycerin	Carl Roth
Tris-Base	Sigma-Aldrich
$LiOAc{\cdot}2H_2O$	Sigma-Aldrich
Sorbitol	Carl Roth
PEG 3350	Sigma-Aldrich
Boric acid	Serva
Rubidium chloride	Sigma-Aldrich
Bacto peptone	Becton Dickinson
Bacto yeast-extract	Becton Dickinson
Agar	Becton Dickinson
Bacto trypton	Becton Dickinson
Adenine	Sigma-Aldrich
Ampicillin	Carl Roth
Bacto-yeast nitrogen base without amino acids	Becton Dickinson
Alanine	Merck
Asparagine	Merck

Arginine	Merck
Aspartatic acid	Sigma-Aldrich
Cysteine	Merck
Glutamine	Merck
Glutamic acid	Sigma-Aldrich
Glycin	Merck
Inositol	Alfa Aesar
Isoleucine	Calbiochem
Lysine	Merck
Methionine	Merck
para-Aminobenzoic acid	Merck
Phenylalanine	Merck
Proline	Merck
Serine	Merck
Threonine	Merck
Tyrosine	Merck
Valine	Merck
Histidine	Merck
Leucine	Merck
Uracil	Merck
Tryptophan	Merck
ClonNAT	Werner BioAgents
Hygromycin	Roche
Sucrose	Sigma- Aldrich
Bromphenol blue	Carl Roth

2.1.2. Devices and commercial kits

Table 2: Devices and commercial kits used for the experiments

Products	Supplier
Tubes 1,5 mL; 2,0 mL	Eppendorf
PCR tubes 0,15 mL	Eppendorf
Pipet tips	Peske
10 mL; 50 mL Falcons	Sarstedt
Culture dishes	Greiner Bio-One
Slide	Menzel
Coverslip 20x20 mm	Menzel
Parafilm „M”	American National Can™
Lens paper	Schütt Labortechnik
E.Z.N.A. Plasmid Miniprep KitI	Omega Bio-tek
Wizard®SV Gel and PCR clean up system	Promega

2.1.3. Equipment

Table 3: Equipment used for experiments

Instrument	Producer
Microliter centrifuge Galaxy 16DH	VWR International
Centrifuge Heraeus Pico 17	Thermo Electron Corporation
Refrigerated centrifuge Heraeus Fresco 17	Thermo Electron Coporation
Refrigerated centrifuge Biofuge primo R	Heraeus
Incubator shaker innovaTM 4230	New Brunswick Scientific
Incubator Heraeus Function Line	Thermo Electron Corporation
Refrigerator 2- 8°C	Liebherr
Freezer -20°C	Beko
Freezer -80°C	New Brunswick Scientific
T100 Thermal Cycler	BioRad
Thermocycler PXE 0.2	Thermo Electron Corporation
Vortex-shaker	VWR International
Microwave	Severin
Transilluminator®, dark reader	Clare chemical research
NanoDrop 2000c	Thermo Scientific
UNITWIST 3D Shaker	UniEquip

2.1.4. Cell strains

The BY4741 yeast strains (genotype Mat a; *his3Δ1; leu2Δ0; met15Δ0; ura3Δ0*) were received from the GFP-library of the "European Saccharomyces cerevisiae Archives for Functional Analysis".

Table 4: Cell strains used for the experiments

Background	Tagged gen	Systematic name	Tag	Marker
BY4741	Sec3	YER008C	GFP	Histidin (-HIS)
BY4741	Sec5	YDR166C	GFP	Histidin (-HIS)
BY4741	Sec6	YIL068C	GFP	Histidin (-HIS)
BY4741	Sec8	YPR055W	GFP	Histidin (-HIS)
BY4741	Sec10	YLR166C	GFP	Histidin (-HIS)
BY4741	Sec15	YGL233W	GFP	Histidin (-HIS)
BY4741	Exo70	YJL085W	GFP	Histidin (-HIS)
BY4741	Exo84	YBR102C	GFP	Histidin (-HIS)
BY4741	Cse4	YKL049C	GFP	Histidin (-HIS)

2.1.5. Enzymes

Table 5: Enzymes used for the experiments

Enzyme	Supplier
EcoRV	New England BioLabs
BglII HF	New England BioLabs
XhoI HF	New England BioLabs
PstI HF	New England BioLabs
BamHI HF	New England BioLabs
NotI HF	New England BioLabs
AlwNI	New England BioLabs
AatII	New England BioLabs
T4 DNA Ligase	New England BioLabs
F- 530 L Phusion® DNA polymerase	Finnzymes
RNase A	Corporation

Table 6: Enzyme Buffers used for the experiments

Enzyme Buffer	Supplier
5x Phusion HF	Finnzymes
NEBuffer 3	New England BioLabs
NEBuffer 4	New England Biolabs

2.1.6. Oligonucleotides

- The plasmids for direct tagging were generated by the M. Knop lab [20].

Table 7: Plasmids used for the experiments

Name	Alias	Tag	Target plasmid	Marker
pYM40	RWC 233	yeGFP	pKS133	Hygromycin (hphNTI)
PYM40	RWC 867	mKate2	pKS133	Hygromycin (hphNTI)
pYM42	RWC 868	mKate2	pKS134-1	Nourseothricin (natNT2)

- DNA standard

Table 8: DNA standard used in the experiments

Product	Supplier
Gene Ruler™ DNA Ladder Mix	Fermentas
Quick-Load® Low Molecular Weight DNA ladder	New England BioLabs

- Primer

Table 9: Primer used for the experiments

Name	Alias	Sequence (5´- 3´)	Function
5´- mKate2- PstI	RWS2121	CTGCAGATGGTGAGCGAGCTGATTAAG	Cloning
3´- mKate2- BHI	RWS2122	GGATCCTCTGTGCCCCAGTTTGCTAG	Cloning
Sso1 5´Prom	RWS1354	CTCGAGCCCACACACTAACGACAAAAGAC	Cloning
Sso1 3´Prom	RWS1355	CTGCAGTTGATTTGTTTCTATTTTTAATTGC	Cloning
Sso1 5´Gen	RWS1356	GGATCCATGAGTTATAATAATCCGTAC	Cloning
Sso1 3´Gen	RWS1357	GCGGCCGCTTAACGCGTTTTGACAACGG	Cloning
Sec3 S2	RWS1065	CTTAATTAGTCTAAATATGTAATATGAAGCGACAATGCAGAGGTTACTTAATCGATGAATTCGAGCTCG	Direct tagging
Sec3 S3	RWS1066	GCTTCACGAAGAACGATATCATAAGTGCGTTCGAGGAATACAAGAATGCCCGTACGCTGCAGGTCGAC	Direct tagging
S3- Sec5	RWS1421	GTATCTGCCAATTTAAAAAGAACTGCTATTCAATTCGCCGCCTTCAGCCGTACGCTGCAGGTCGAC	Direct tagging
S2- Sec5	RWS1427	CGATTTGTGTTAATAATCATTGTTAGTACATCTTTATACCTCTGTTTCTAATCGATGAATTCGAGCTCG	Direct tagging
Sec6 S2	RWS1370	CTATACTATGTTATATGTAATCAGTGAACTTTTTTTTTTTCTTGTATATCGTTAATCGATGAATTCGAGCTCG	Direct tagging
Sec6 S3	RWS1371	GTGGATCGCGAACCTACTTTGATGAGGCGGTTTGTATTAGAATTCGAAAAGCAACGTACGCTGCAGGTCGAC	Direct tagging
S3- Sec8	RWS1422	GGAAAACTTAAAAGCAAATTGAATGCTGTCCATACTGCAAACGAAAAACGTACGCTGCAGGTCGAC	Direct tagging
S2- Sec8	RWS1428	CATTCATTTATTTATCAAATTAATTTTACACAAACTAAAAATGTCAATCGATGAATTCGAGCTCG	Direct tagging

S3- Sec10	RWS1423	GGACTTCAATCATGACAATTTCATTAATAGCGTTAAATTGAATTTTAGACGTACGCTGCAGGTCGAC	Direct tagging
S2- Sec10	RWS1429	CTCAAAAAAGGCATTCTGCCAAAAAACGTGAATACTCTATGTACGCTAATCGATGAATTCGAGCTCG	Direct tagging
S3- Sec15	RWS1004	GTGTCATTGACTCTAATACGAGTAGGATAGCCAAATTTTTTAATAGACGTCGTACGCTGCAGGTCGAC	Direct tagging
S2- Sec15	RWS1005	TTCTTTCTTATGAACGTACAAATGATTATACTGAGATAATATCTAATTTTATCGATGAATTCGAGCTCG	Direct tagging
S3- Exo70	RWS1002	TCAAATATACCCCTGACGAACTAACTACTGTTCTTAACCAATTAGTGAGACGTACGCTGCAGGTCGAC	Direct tagging
S2- Exo70	RWS1003	TGGTACGTTCTTTTCTTTAATTTTGCTTTTGAAAAGTGATGTTCGCAATATCGATGAATTCGAGCTCG	Direct tagging
S3- Exo84	RWS1424	CTACAAATTGGACGAGTTTATCAAAAAGAACAGTGATAAAATTCGCCGTACGCTGCAGGTCGAC	Direct tagging
S2- Exo84	RWS1430	CACATCATATATATTGAAGTGAGGTTTATTTTCTGTGATCTTGTTTAATCGATGAATTCGAGCTCG	Direct tagging
Cse4 S3	RWS2112	GAATTACTATAATGAAGAAAGACATGCAACTAGCAAGAAGAATCAGGGGACAGTTTATTCGTACGCTGCAGGTCGAC	Direct tagging
Cse4 S2	RWS2113	CAATATAAACCCCGAAAAAGGGAAAAATCGGCTCCAGCCCTGAAGCACAAATATCACTAATCGATGAATTCGAGCTCG	Direct tagging
Sec3 forward	RWS2151	GCATATAGCAGGCAGAACCTAG	Colony PCR
Sec3 reverse	RWS2152	CTCGGACGAATCCTCACTGATATGC	Colony PCR
Sec5 forward	RWS2153	GGCCTCAGCTCATCCATAAG	Colony PCR
Sec5 reverse	RWS2154	CGAATTTGACAGTGCCATCA	Colony PCR
Sec6 forward	RWS2155	CTGGGACTCGCGCATAGATTTAC	Colony PCR
Sec6 reverse	RWS2156	CTAGACGGGAATACTGCCTGG	Colony PCR
Sec8 forward	RWS2157	GAATTACCGCATTGTTCTGTCG	Colony PCR
Sec8 reverse	RWS2158	CCATTTCTGATTGCTTCGCTTC	Colony PCR
Sec10 forward	RWS2159	CATTGGCGGTGTTGTAGTTACG	Colony PCR
Sec10 reverse	RWS2160	GTTGAGAAGGTATGCCAGGTGG	Colony PCR

Sec15 forward	RWS2161	GAATTAGACAGGAAGATGCGGCTC	Colony PCR
Sec15 reverse	RWS2162	CGTGTGCAGACAGACATACTTTC	Colony PCR
Exo70 forward	RWS2163	GATTGGAACGGCTGAAGAAACG	Colony PCR
Exo70 reverse	RWS2164	GAGTACCCTTTAGTCTAGCACAAG	Colony PCR
Exo84 forward	RWS2165	CCTAGTAGATTGGTGTAGCGACG	Colony PCR
Exo84 reverse	RWS2166	CCAGAAGATTCCAGTCCAAGAG	Colony PCR
nat forward	RWS2167	CCTGTAGGTCAGGTTGCTTTC	Colony PCR
hyg forward	RWS2168	GGAAGGAGTTAGACAACCTGAAG	Colony PCR
yeGFP reverse	RWS2170	CTAAGGTTGGCCATGGAACTGG	Colony PCR
mKate2 reverse	RWS2171	CAGGATGTCGAAGGCGAAGG	Colony PCR
Cse4 forward	RWS2172	GATCAGGATTTACGTTGGCAG	Colony PCR
Cse4 reverse	RWS2173	CCTTTGATTTGGAGCTTCATCG	Colony PCR

2.1.7. Buffers and Solutions

Table 10: Buffers and solutions used for the experiments

1x TE- Buffer pH= 8.0	
1.21 g	Tris-base
0.37 g	Na_2-EDTA·$2H_2O$
Ad 1000 mL	ddH_2O
SORB pH= 8.0	
100.0 mL	1 M LiOAc (f.c. 100 mM)
10.0 mL	1 M Tris- HCl pH= 8.0 (f.c. 10 mM)
2.0 mL	0,5 M EDTA/ NaOH pH= 8.0 (f.c. 1 mM)
500.0 mL	2 M Sorbitol (f.c. 1 M)
Ad 1000.0 mL	ddH_2O
Adjusted to pH 8.0 with acetic acid	
PEG- Mix	
10.0 mL	1 M LiOAc (f.c. 100 mM)
1.0 mL	1 M Tris- HCl pH= 8.0 (f.c. 10 mM)

0.2 mL	0.5 M EDTA/ NaOH pH= 8.0 (f.c. 1 mM)
40.0 g	PEG 3350 (f.c. 40 %)
Ad 100.0 mL	ddH_2O
10x TBE- Buffer	
108.0 g	Tris-Base (f.c. 440 mM)
55.0 g	Boric acid (f.c. 440 mM)
40.0 mL	2.0% (v/v) 0.5 M EDTA pH= 8.0 (f.c. 10mM)
1000.0 mL	ddH_2O
Lysis-Buffer	
2.0 mL	Triton X-100 (f.c. 2%)
10.0 mL	10% SDS (f.c. 1%)
10.0 mL	1 M NaCl (f.c. 100 mM)
1.0 mL	1 M TrisHCl pH= 8.0 (f.c. 10 mM)
0.2 mL	0.5 M EDTA (f.c. 1 mM)
Ad 100 mL	ddH_2O
20% Glucose	
100.0 g	Glucose
Ad 500 mL	ddH_2O
6x loading dye	
250 mL	40% Sucrose
0.5 g	Bromophenol blue

2.1.8. Media

Table 11: Media used for the experiments

YP-Medium		
16.0 g	Bacto peptone	
8.0 g	Bacto yeast-extract	
0.004 g	Adenin	
Ad 1000 mL	ddH_2O	
YT- Medium		
8.0 g	Bacto trypton	
5.0 g	Bacto yeast-extract	
5.0 g	NaCl	
Ad 1000 mL	ddH_2O	
+ Amp (100 µg/mL)	0.4 mL	Amp stock solution (100 mg/mL)
SC all		
6.7 g	Bacto- yeast nitrogen base without amino acids	
2.0 g	SC-all drop out powder	
Ad 1000 mL	ddH_2O	

SC-His-Trp-Leu-Ura-Ade drop out pulver		
20 g	Alanine	
20 g	Asparagine	
20 g	Arginine	
20 g	Aspartatic acid	
20 g	Cysteine	
20 g	Glutamine	
20 g	Glutamic acid	
20 g	Glycine	
20 g	Inositol	
20 g	Isoleucine	
20 g	Lysine	
20 g	Methionine	
2 g	para- Aminobenzoic acid	
20 g	Phenylalanine	
20 g	Proline	
20 g	Serine	
20 g	Threonine	
20 g	Tyrosine	
20 g	Valin	
SC-all drop out pulver		
36.7 g	SC-His-Trp-Leu-Ura-Ade drop out pulver	
2.0 g	Histidine	
4.0 g	Leucine	
2.0 g	Uracil	
2.0 g	Tryptophan	
0.5 g	Adenine	
YT plates		
8.0 g	Agar	
3.2 g	Bacto trypton	
2.0 g	Bacto yeast-extract	
2.0 g	NaCl	
Ad 400 mL	ddH_2O	
+ Amp (100 µg/mL)	0.4 mL	Amp stock solution (100 mg/mL)
SCD		
45 mL	SC all solution	
5 mL	Glucose solution 20%	
YPD		
45 mL	YP solution	
5 mL	Glucose solution 20%	
YPD-plates		
8.0 g	Bacto peptone	

	4.0 g	Bacto yeast-extract
	22 mg	Adenin
	360 mL	ddH_2O
	8.0 g	Agar
	40 mL	Glucose solution 20%
+ NAT (100 µg/ mL)	0.2 mL	ClonNAT solution (200 mg/mL)
+ Hygromycin (300 µg/ mL)	2.4 mL	Hygromycin solution (50 mg/ mL)

2.1.9. Software

Table 12: Software used for the experiments

Software	Function	Supplier
A plasmid Editor (ApE) v2.0.45	Plasmid editing	M. Wayne Davis
Origin®8.5	Data plotting	OriginLab Corporation
Excel 2010	Collecting data	Microsoft
ImageJ 1.47a	Video processing	Wayne Rasband, National Institutes of Health
Live Acquisition	Microscope controlling	Till Photonics

2.2.Methods

2.2.1. N- terminal tagging

Yeast genomic DNA preparation

The yeast strain BY4741 was inoculated overnight in 10 mL YPD- media at 30°C. Cells were harvested at 3000 rpm for 3 minutes at room temperature. The supernatant was discarded and the remaining pellet was washed with 3 mL ddH_2O. The cell pellet was resuspended in 600 µL lysisbuffer and split into three aliquots 200 µl each. In every tube was added 200 µL Phenol/ Chloroform, 200 µL TE-Buffer pH= 8.0 was added and the same volume of glass beads. After vortexing the tubes for 7 min, they were centrifuged with 14000 rpm for 8 min at room temperature. The upper layer of the solution was transferred into a new tube. Then the solution was inverted four times after adding 1 mL absolute ethanol and centrifuged with 14000 rpm for 2 min at room temperature. The supernatant was discarded and the DNA- Pellet was washed with 700 µL absolute Ethanol. The dried pellet was dissolved in 75 µl TE-RNAse free buffer.

Primer design

The SGD Database was used to obtain the sequences of the genes. The primers should have a length between 22 to 30 nucleotides and a melting temperature of 56°C. Better annealing during the PCR is supported by primer starting and ending with G or C. For integration of the gene sequences in a tagging vector restrictions site are needed. Therefore the forward primer was flanked by a restriction site at the 5' end and the reverse primer was flanked by a restriction site at the 3' end. The region 250- 400 bp upstream of the gene was used as a promoter sequence. The primers were diluted to a final concentration of 10 pmol/µL.

Gene amplification via polymerase chain reaction (PCR)

Genes were amplified by PCR using Phusion DNA polymerase with 3'-5' exonuclease activity. A hot start was performed to avoid primer degeneration by polymerase. The PCR reaction mix had a total volume of 50 µL which was filled in PCR tubes and consisted of:

36.5 µL	ddH_2O
10 µL	5x Phusion Buffer HF
1 µL	dNTPs (10 nM)
1 µL	Genomic DNA
0.5 µL	Forward primer
0.5 µL	Reverse primer
0.5 µL	Phusion DNA polymerase

Cloning PCR amplification program:

98°C	3 min
Phusion DNA Polymerase was added	
98°C	10 sec
55°C	30 sec
72°C	35 sec
72°C	7 min
12°C	∞

Agarose gel electrophoresis

PCR product was tested for purity and unspecific fragments by analytical agarose gel electrophoresis.

Contents 1% agarose gel:

0.5 g	Agarose powder
50 mL	1x TBE buffer
5 µL	Ethidiumbromid (1%)

Probe loading:

50 µL	PCR product
10 µL	6x loading dye

The gel was running at 100V for 30 min. To illuminate and to excise the DNA fragments labeled with ethidiumbromid a transilluminator was used. The sizes of the DNA fragments were determined by comparison to the "gene ruler DNA ladder mix". Excised fragments were isolated and purified using the "Wizard®SV Gel and PCR Clean-Up System".

Producing pJET1.2- backbone and ligation

As a backbone for the DNA fragments the pJET1.2 plasmid was used. This plasmid contains a β-lactamase gene conferring resistance to ampicillin which is used for selection and maintenance of *E.coli* cells. Furthermore, the plasmid contains the lethal gene eco47IR, coding for the Eco47I restriction endonuclease, and enabling positive selection of the recombinants. To prepare the plasmid for ligation it has to be digested with EcoRV to eliminate the function of the lethal gene and to obtain blunt ends enabling the ligation with the DNA fragments which also had blunt ends, because during a PCR only blunt ends can be produced.

pJET1.2- plasmid digestion:

5 µL	Plasmid
3 µL	10x BSA
3 µL	10x NEB Buffer 3
1 µL	EcoRV
18 µL	ddH_2O

The reaction mixture was incubated at 37°C for 2 - 3 h.

Ligation:

1 µL	T4 DNA ligase buffer
2 µL	Digested pJET1.2
6 µL	DNA fragment
1 µL	Ligase

The reaction mixture was incubated at room temperature for 1 h.

Transformation of E. coli cells

Amplification of the DNA Fragment inserted in pJET1.2 was carried out in *E.coli* cells. Before starting transformation the *E.coli* cells of the strain DH5α were treated with $RbCl_2$ to induce competence. Cells were stored at -80°C. 50 µL competent E.coli cells were added to each ligation reaction mixture kept on ice for 25- 28 min. Cells were heated to 42°C for 2 min, chilled to 4°C for 2 min and 100- 150 µL YT medium was added. The culture was plated onto YT- ampicillin plates and incubated at 37°C overnight.

Plasmid preparation

A colony was picked from the plate with a sterile pipette tip and inoculated in 3.5 mL YT- ampicillin at 37°C overnight. The plasmid preparation was performed using the "E.Z.N.A. Plasmid Miniprep Kit" and according to its instructions.

Test digestion and sequencing

The size of DNA fragments was determined using analytical gel electrophoresis.

Test digestion:

3 µL	Plasmid
2 µL	10x BSA
2 µL	Buffer 3
1 µL	BglII restriction enzyme
12.5 µL	ddH_2O

The reaction mixture was incubated at 37°C for 1 h before loading it on a 1% agarose gel.

Probe loading:

10 µL	Reaction mixture
2 µL	6x loading dye

Sequencing of the plasmids was carried out to verify the right direction and sequences of the insert. The sequencing was done by the Biochemistry Core Facility. They used Modified Sanger dideoxy terminator cycle sequencing chemistry.

Sequencing:

3.5 µL	ddH_2O
1 µL	Per 3' and 5' Primer
3 µL	Plasmid

Double digestion

The next step was to double digest the pJet1.2 plasmids containing the DNA fragment and to double digest the pTL58 plasmid to obtain the backbone for the following ligation.

Plasmid	alias	Restriction enzymes
pTL 58	RWC 352	XhoI HF + NotI HF
pJET1.2 pSSO1	RWC 867	XhoI HF + PstI HF
pJET1.2 SSO1	RWC 868	BamHI HF + NotI HF
pJET1.2 mKate2	RWC 869	PstI HF + BamHI HF

Double digestion:

19 µL	ddH_2O
3 µL	Buffer 4
3 µL	10x BSA
3 µL	Plasmid
1 µL	Of each enzyme (e.g. XhoI HF + NotI HF

The reaction mixture was incubated at 37°C for 2- 3 h.

The double digestion reaction mixtures of pTL58, pJET1.2 SSO1 and pJET1.2 mKate2 were loaded on a 1% agarose gel. The pJET1.2 pSSO1 was checked on a 2% agarose gel to separate two fragments with similar length properly because the double digestion with XhoI and PstI produces two fragments with similar length. In addition a low molecular weight DNA ladder was used to determine the length of the fragments with more accuracy. For this electrophoresis sybr green Instead of ethidiumbromid

was used to mark the DNA fragments because the fragments marked with sybr green can be seen superiorly with the transilluminator.

Contents 1% agarose gel:

0.5g	Agarose powder
50 mL	1x TBE Buffer
5 µL	Sybr Green

Contents 2% agarose gel:

1.0 g	Agarose powder
50 mL	1x TBE Buffer
5 µL	Sybr Green

Correct fragments were excised of the gels, isolated and purified as described in chapter 4.

Ligation with pTL58 plasmid

Concentration of the purified fragments was determined using the NanoDrop2000c prior ligation to calculate the amount which had to be used for the ligation reaction mixtures.

Fragment	Concentration
pTL58 backbone	13.3 ng/µL
pSSO1	5.7 ng/µL
SSO1	3.9 ng/µL
mKate2	3.8 ng/µL

Ligation reaction mixture calculation:

The different lengths of the fragments have to be taken in account for calculation. The ratio between the pTL58 backbone and the fragments should be 1:3.

Fragment	Backbone pTL58	pSSO1	SSO1	mKate2
Length [kb]	5.94 kb	0.33 kb	0.88 kb	0.7 kb
Mass [µg]	100	16.68	44.4	35.4
Volume [µL]	7.5	2.9	11.4	9.3

The volume for the backbone pTL58 was calculated with following formula:

$$Vol(backbone\ pTL58) = \frac{m(backbone\ pTL58)}{c\ (backbone\ pTL58)}$$

The volume of the fragments was calculated with following formula:

$$Vol(pSSO1) = \frac{m(backbone\ pTL58) \cdot l(pSSO1) \cdot 3}{l(backbone\ pTL58) \cdot c(pSSO1)}$$

Vol= volume

m= mass

l= length

c= concentration

Values for the volume SSO1 and mKate2 were calculated corresponding to the previous calculation.

Final ligation reaction mixture for 20 µL:

2.0 µL	T4 DNA ligase buffer
1.0 µL	T4 DNA ligase
4.1 µL	pTL58 backbone
1.6 µL	pSSO1
6.2 µL	SSO1
5.1 µL	mKate2

The reaction mixture was incubated at 16°C overnight. The ligated plasmid is transformed in *E.coli*.

Control digestion

After plasmid preparation was conducted ligation was tested by a control digest.

Control digestion:

3.0 µL	Plasmid
2.0 µL	Buffer 4
2.0 µL	10x BSA
1.0 µL	Aat II (restriction enzyme)
1.0 µL	Alw N I (restriction enzyme)
11 µL	ddH_2O

The reaction mixture was incubated at 37°C for 1.5 h and correct size of the fragment was analyzed using analytical agarose gel electrophoresis.

2.2.2. C- terminal direct tagging

2.2.2.1. Tagging of yeast gene

Homologous recombination is very efficient and can be used for genomic integration of fluorophores. Amplification of chosen resistance cassettes was carried out according to Janke, Magiera [20]. The amplified PCR product was used for transformation of yeast cells, as described in chapter 2.2.2.4. After the yeast cell has taken up the PCR product, homologous recombination can take place which results in the insertion of the PCR product into the genome.

2.2.2.2. Primer design

Two primers, the S2-primer and the S3-primer which contain homologues sequences, were needed to amplify the resistance casette. To construct the S2-primer the reverse complement of 45-55 bases downstream of the STOP-codon, including the stop codon, of the gene is flanked by 5'-ATCGATGAATTCGAGCTCG-3'. The S3-primer contains 45-55 bases upstream the STOP-codon, excluding the STOP-codon, of the gene flanked by 5'-CGTACGCTGCAGGTCGAC-3'[20]. Primers should end with one to two guanine nucleotides or cytosine nucleotides.

2.2.2.3. PCR reaction mixture and amplification program

For the PCR following reaction mixture was used:

0.5 µL	S2-primer
0.5 µL	S3-primer
1.0 µL	Phusion DNA polymerase
1.0 µL	dNTPs
10.0 µL	5x Phusion HF-Buffer
1 µL	Plasmid 1:100
36 µL	ddH_2O

Amplification program for plasmids with a hphNTI resistance [20]:

95°C	3-4 min
Phusion DNA Polymerase was added (hot start)	
95°C	30 sec
54°C	30 sec
68°C	2 min 40 sec
72°C	35 sec
95°C	30 sec
54°C	30 sec
68°C	2 min 40 sec (+ 20 sec/ cycle)
12°C	∞

Amplification program for plasmids with natNT2 resistance [20]:

97°C	3-4 min
Phusion DNA Polymerase was added (hot start)	
97°C	1 min
54°C	30 sec
68°C	2 min 40 sec
72°C	35 sec
97°C	1 min
54°C	30 sec
68°C	2 min 40 sec (+ 20 sec/ cycle)
12°C	∞

The PCR product was identified and separated in a 1% agarose gel. Afterwards the required fragments were excised and purified with the "Wizard®SV Gel and PCR Clean-Up System". The illumination of the bands should not be done with an UV-light because the UV radiation can destroy the ends of the PCR product or causes mutations like thymine dimers.

2.2.2.4. Transformation of yeast cells

A colony was picked with a sterile pipette tip from a plate and inoculated in 6 mL YPD- medium in an agitating incubator at 30 °C overnight. The cell suspension was filled in a 1.5 mL tube and was pelleted with a centrifuge at 0.5 g for 5 min. After this step the supernatant was discarded. This step was repeated until the cell pellet was about 5 mm high. Then the cell pellet was washed for 5 min at 0.5g with 1mL ddH_2O. The supernatant was discarded and the remaining cell pellet was resuspended in 1 mL SORB. Afterwards the cell suspension was centrifuged with 0.5 g for 5 min, the supernatant was discarded and the pellet was resolved in 80 µL SORB. This cell suspension was kept on ice. First 15 µL PCR product was put in a tube, followed by 50 µL SORB-cell suspension and 5 µL ssDNA, which was activated for 5 min at 96 °C before and then kept on ice. Finally 300 µL PEG mix was added and the whole suspension was mixed with a pipette immediately and carefully. After that the suspension was incubated at 30°C for 1h.

After 1 h 35 µL DMSO was added to the cell suspension. To heat shock the cells they were incubated at 42 °C for 15 min. Then the cells were spun at 0.5 g for 5 min and the supernatant was discarded before resuspending the cell pellet in 1 mL YPD- medium. The culture was incubated at 30°C for 6 – 8 h, when natNT2 resistance was incorporated, or for 8 – 10 h, when hphNTI resistance was incorporated, to make sure the cells could develop their antibiotic resistance. The last step was to plate the cells onto an appropriate plate and incubate it at 30 °C. After approximately two days visible colonies were picked from the plates with a sterile pipette tip and transferred to a new equal plate.

2.2.3. Colony PCR

Primer design

Primers should have a length between 18- 30 nucleotides and a melting temperature between 54 – 56°C. Furthermore they should have guanine nucleotides or cytosine nucleotides at the 3’ and 5’ ends.

PCR reaction mixture and amplification program

The former existence of the GFP in genome was checked first with one primer combination. Secondly the correct integration of the cassette was tested with two different primer combinations. A forward primer of the gene and reverse primer of the fluorophore were designed to check the connection

between the end of the gene and the fluorophore. The connection between the sequence downstream the gene and the resistance gene was examined with a forward primer of the resistance sequence and a reverse primer of the sequence downstream the gene.

Colony PCR:

36.5 µL	ddH_2O
10 µL	5x Phusion HF- Buffer
1 µL	dNTPs
1 µL	Forward primer
1µL	Reverse primer
Small amount of the colony	
0.5 µL	Phusion DNA polymerase

Colony amplification program:

98°C	35 min	ffff
Add Phusion DNA polymerase (hot-start)		
98°C	15 sec	
55°C	45 sec	
72 °C	1 min	
72°C	5 min	
12°C	∞	

10 µL PCR product mixed with 2 µL 6x loading dye was loaded into a 1% agarose gel. The fragments in the gel verified the right insertion of the fluorophore tag.

2.2.4. Data acquisition for lifetime of single color strains

To analyze the spatio and temporal organization of the exocyst complex, we measured the lifetimes of four individual exocyst subunits at the plasma membrane. The strains Sec3-GFP, Exo70-GFP, Sec6-GFP and Sec8-GFP were obtained from the GFP library. To achieve maximum reproducibility all conditions were standardized and experiments conducted at the same day. The strains were illuminated with a 488 nm laser.

Table 13: recording settings for exocytotic patch lifetime measurements at the plasma membrane

Loop	Exposure	Cycle time	488nm laser intensity
250	50 ms	250 ms	100%

Only the TIRF angle had to be adjusted for each cell hence it depends on the exact location of the cell depends on the thickness of the coverslip, for example. The movies were processed for a proper identification of the patches before evaluating them. The image process pipeline is shown in Figure 5.

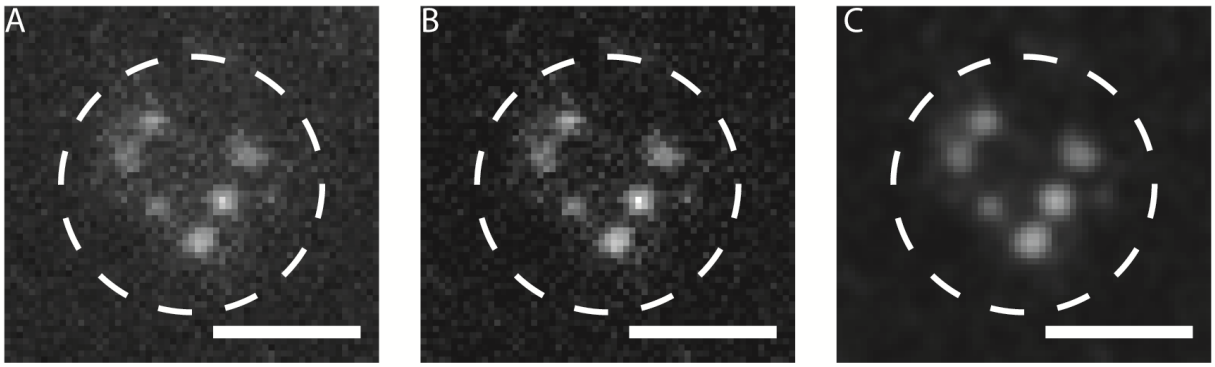

Figure 1: Image processing pipeline

A: Raw image; B: Image with background subtraction; C: Image with Gaussian blur; Scale bar 2 µm

The background subtraction was done with a rolling ball radius of 15 pixels to remove smooth continuous background of the image (Figure 5; B). Therefore ImageJ used an algorithm based on the "rolling ball" algorithm [21]. Afterwards the filter Gaussian Blur was used with a Sigma (Radius) of 1 pixel to smooth the patches further and to reduce image noise for a better identification of the patches. The next step was to generate a maximum projection of all slides to visualize all patches within the movie (Figure 6; B). A ROI (region of interest) line was drawn through all visible patches manually (Figure 6; C); following a kymograph was generated which visualizes the temporal trend against the movement of the patches (Figure 7; E). Line scans of the patches in kymographs were generated to determine the appearance and disappearance of the patches with a maximum of accuracy (Figure 7; A-D). Out of these data the lifetimes could be obtained hence one pixel in the kymograph correlates to the cycle time of 250 ms.

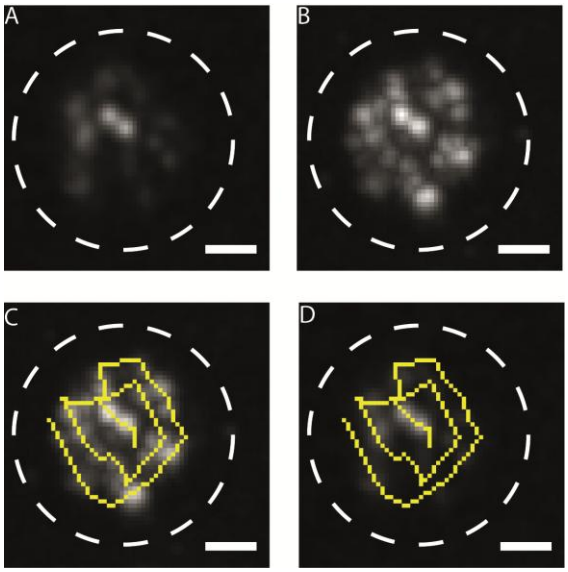

Figure 2: Determination and drawing of the ROI

A: First slide of the movie; B: Maximum projection of the movie; C: Maximum projection with determined ROI; D: First slide of the movie with ROI; Scale bar 1 µm

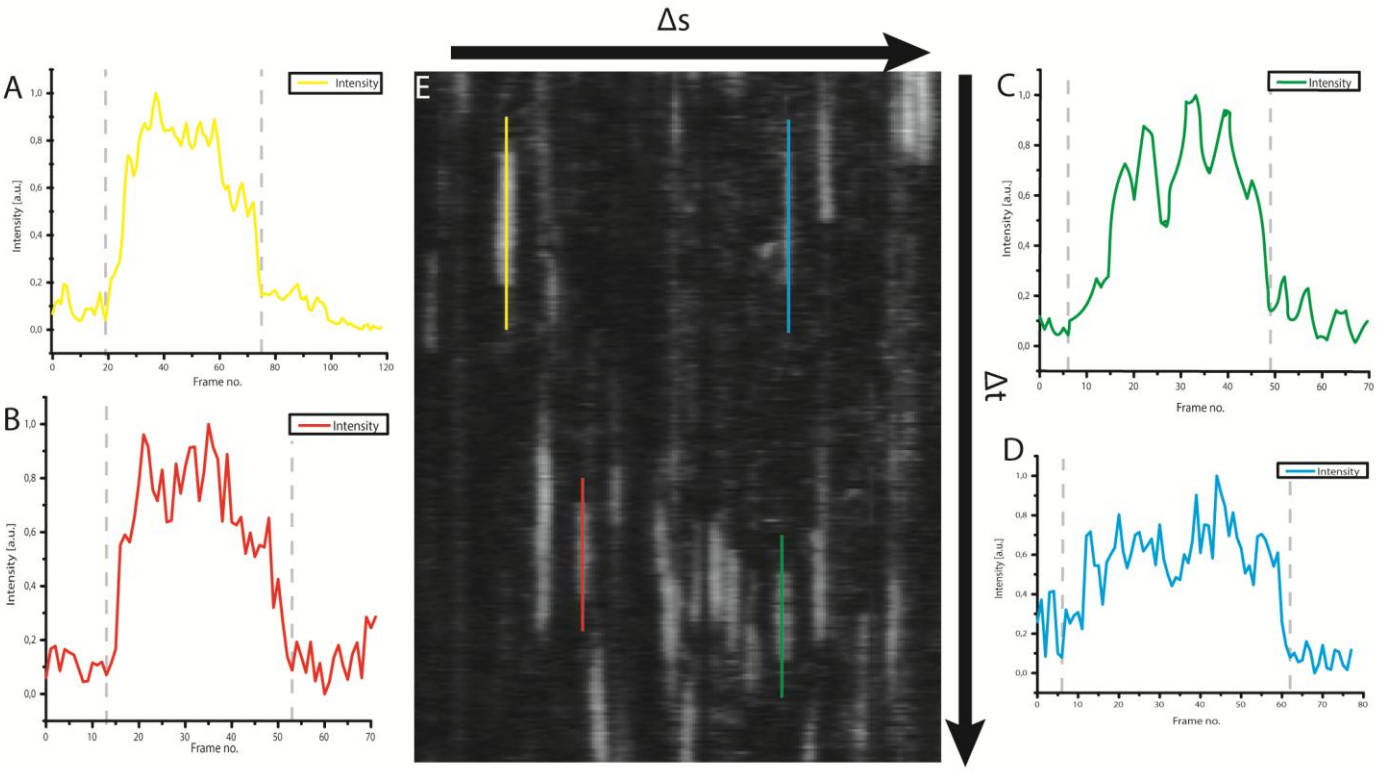

Figure 3: Kymograph and linescans

A – D: Four exemplary linescans of patches detected in the kymograph; E: Kymograph of the cell in figure 6

2.2.5. Data acquisition for lifetime of double color strains

For investigations of the organizaion of the exocyst complex time- resolved colocalizations of two subunits were examined. To tag the proteins the fluorophores GFP and mKate2 were used. GFP was excited with a 488 nm laser and mKate2 was excited with a 561 nm laser. Five different strains (Sec3-GFP with Exo70-mKate2; Exo70-GFP with Sec3-mKate2; Sec6-GFP with Exo70-mKate2; Exo70-GFP with Sec6-mKate2; Sec6-GFP with Sec5-mKate2) were examined.

Only the TIRF angles for the 488 nm laser as well as for the 561 nm laser had to be adjusted for each recording. The other parameters were kept constant. The red channel was always recorded first. The red and green channels were recorded with a dual emission filter to minimize the time passing between recordings of the two channels. This set up resulted in a better time resolution. If we would have used two single emission filters we had to change the filters for recording of green and red channels. This would have lead to an increased recording time of 1.2 sec for each channel.

For the strains Exo70-GFP Sec6-mKate2, Sec6-GFP Exo70-mKate2 and Sec6-GFP Sec5-mKate2 the following settings were used.

Table 14: Settings for double color strain measurements

Loop	Exposure 561 nm	Cycle time 561 nm	561 nm laser intensity
250	50 ms	250 ms	100%

Loop	Exposure 488 nm	Cycle time 488 nm	488 nm laser intensity
250	50 ms	250 ms	100%

For the strains Sec3-GFP Exo70-mKate2 and Exo70-GFP Sec3-mKate2 a time delay of 250 ms was included after recording the green channel.

When the movies were merged one pixel in the kymograph is equivalent to a time of 500 ms for the settings without time delay and 750 ms for the settings with time delay.

Image processing as described in chapter 3.2.1 was conducted. Green and red channels were merged (Figure 9) and linescans generated for each channel individually to determine the lifetime of each patch (Figure 11). With these lifetimes differences the appearance and disappearance of the patches could be determined.

To visualize the process the strain Exo70-GFP with Sec6-mKate2 was used.

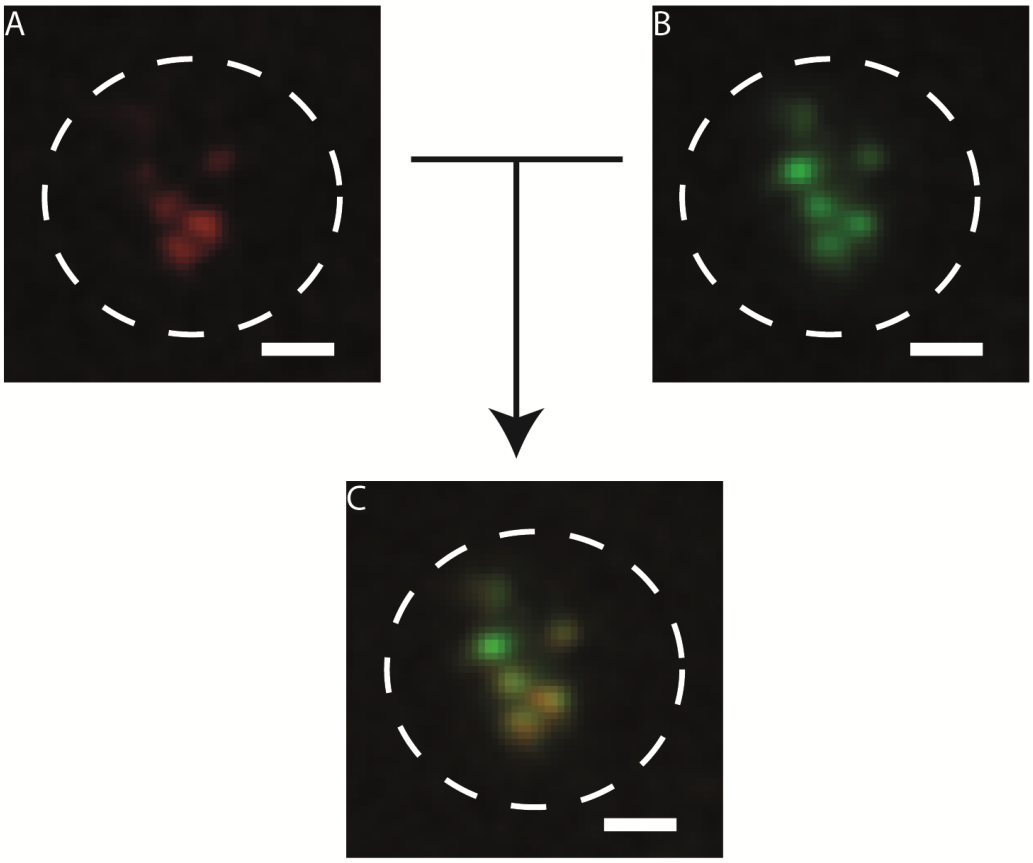

Figure 4: Merge of green and red channels

A: cell in the red channel; B: cell in the green channel; C: Overlay of both channels; Scale bar 1 µm

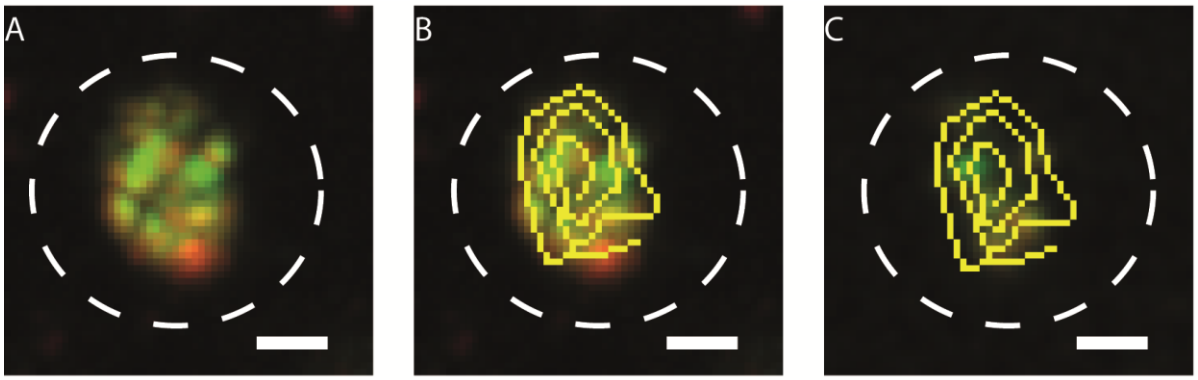

Figure 5: Determination of the ROI

A: Maximum projection of the video; B: Maximum projection of the video with drawn ROI; C: Cell of Figure 9, C with ROI; Scale bar 1µm

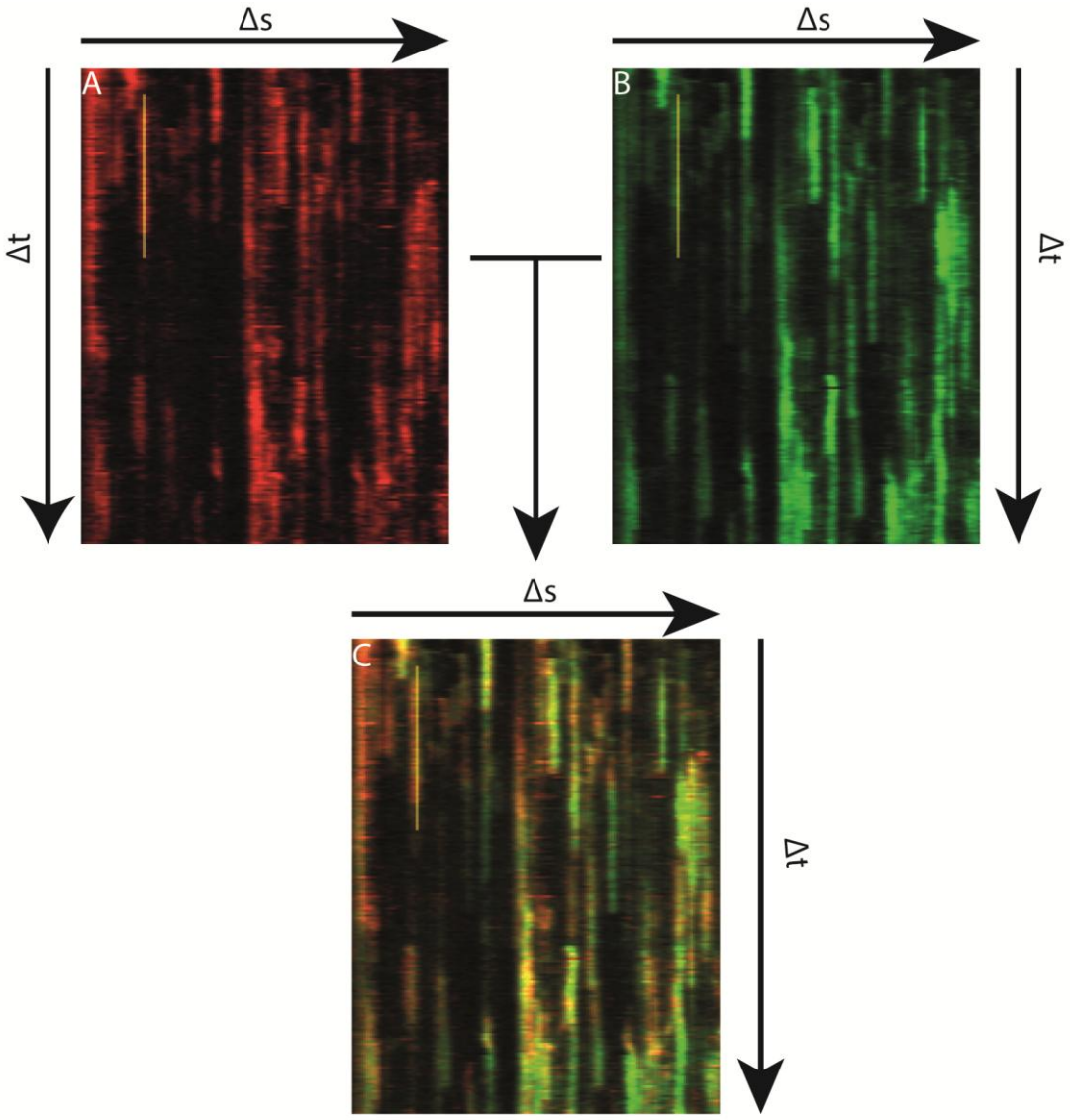

Figure 6: Kyomgraphs of the cell in figure 10; C

A: Kyomgraph of the red channel; B: Kymograph of the green channel; C: Overly of both channels

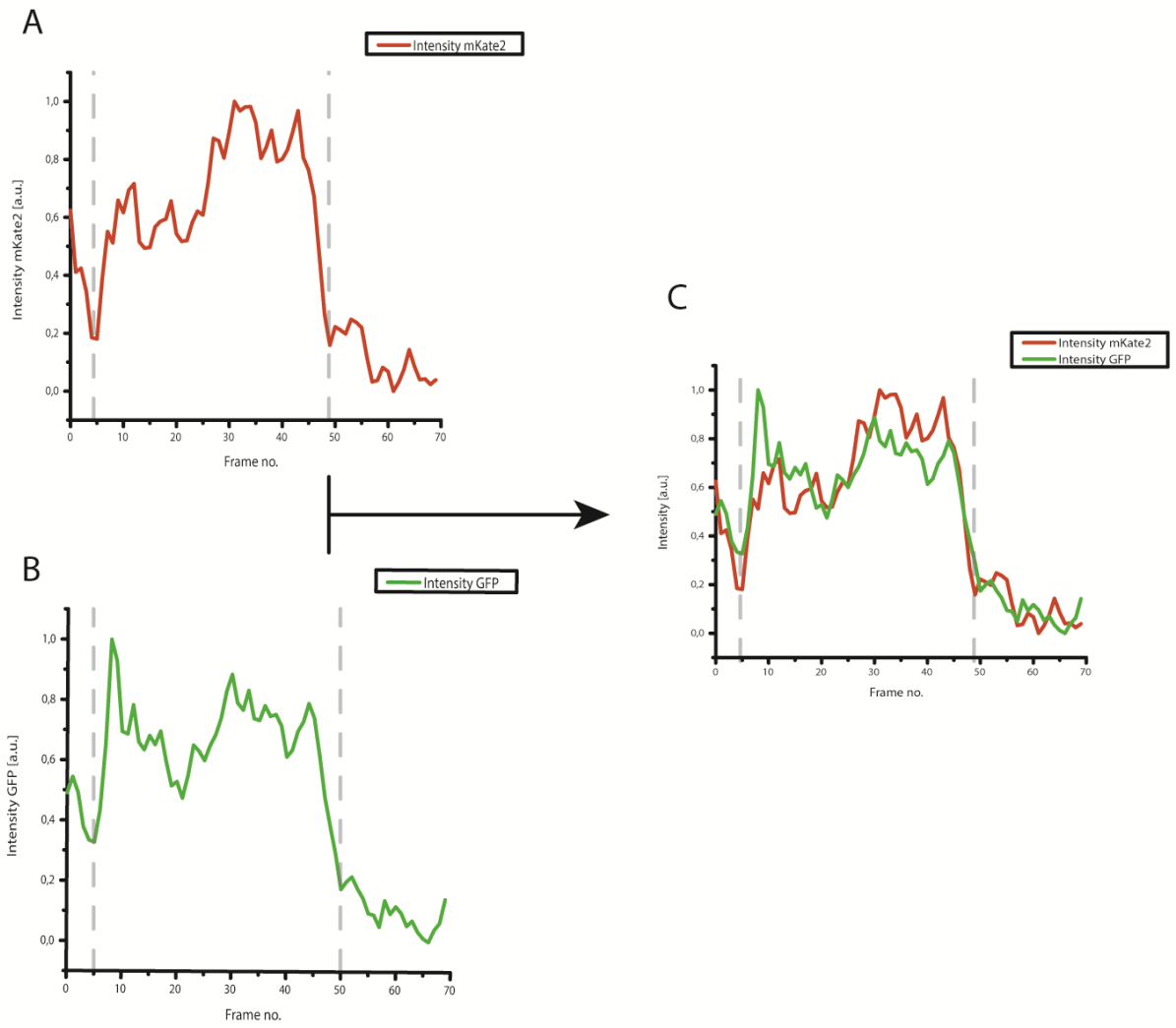

Figure 7: Linescans of patch marked in Kymograph

A: Linescan of the red channel; B: Liescan of the green channel; C: Overlay of the linescans of both channels

2.2.6. Data acquisition for subunit counting with Cse4

To gain comparable results the settings of the microscope were standardized. In this experiment TIRF microscope was not used in TIRF mode, because only the surface of the cell can be observed in this mode, but in epi fluorescent mode as a bright field microscope. Subsequently, the laser was penetrating the sample perpendicular. With this experimental set-up the intensity of the exocyst patches and of Cse4, which is located in the nucleus, could be measured. For recordings a z-stack was

used. During a z-stack recording the focus of the z-plane changed in equal distances with every picture of the movie, subsequently, the whole cell was scanned in z-direction. The microscope settings were collected in the following table.

Table 15: Settings for the quantification experiments

Loop	Z- shift/ loop	Exposure	Cycle time	Time delay	488 nm laser intensity
49- 59	100 nm	100 ms	250 ms	150 ms	100%

The movies for the measurements were recorded of cells in metaphase to late anaphase. The integrated intensities were obtained by using the methods of Hoffman, Pearson [22] and Johnston, Joglekar [23]. First of all a circle of 21 pixel² (A_{ii}) was centered on the fluorescence spot. The area was selected manually to contain all visible intensity of the spot. After that the integrated intensities of all z planes were measured. The maximum value (F_{ii}) and the frame number were noted. Another 35 pixel² (A_{io}) circle was centered on the small circle. This circle was bigger than the small circle but small enough to avoid overlap with another fluorescence spot. Again all integrated intensities of every z plane were measured. The integrated intensity (F_{io}) which belonged to the previous determined frame number was noted. The measured value of the 21 pixel² circle contained the fluorescence of the protein and the local background. To obtain the background component the value of the 21 pixel² circle was subtracted from the value of the 35 pixel² region. This value was scaled in proportion to the 21 pixel² circle and was subtracted from the origin value of the 21 pixel² circle [22]. The process is pictured in Figure 23. The following formula was used to determine the integrated density without local background (F_i). The size of the circles was equal for Cse4 and for the subunits to obtain comparable results.

$$F_i = F_{ii} - (F_{io} - F_{ii}) \times \left(\frac{A_{ii}}{A_{io} - A_{ii}}\right)$$

F_i = integrated intensity without local background

F_{ii} = integrated intensity of the inner circle

F_{io} = integrated intensity of the outer circle

A_{ii} = area of the inner circle

A_{io} = area of the outer circle

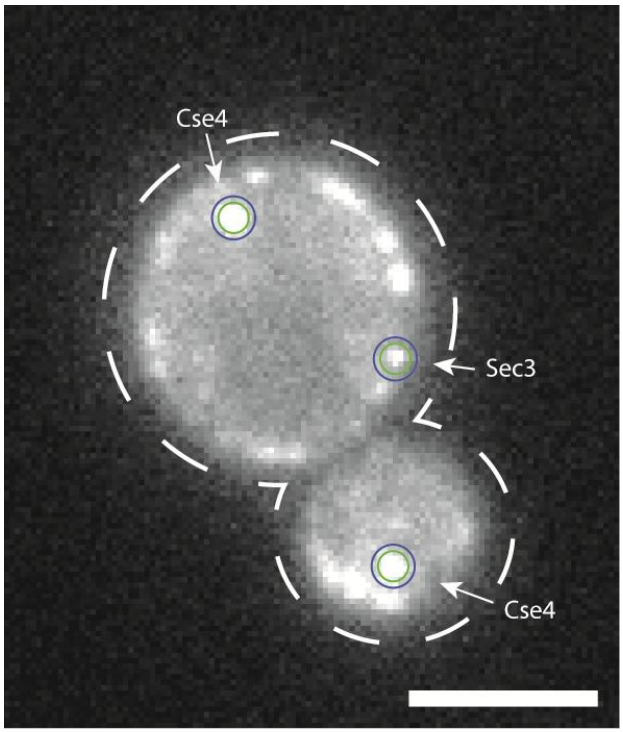

Figure 8: Cse4-GFP Sec3-GFP strain

Both Cse4 spots and one Sec3 spot are marked, further Sec3 spots can be seen at the plasma membrane, Scale bar 3 µm

The intensities of Cse4 and the subunits were measured in the same strains to have the same conditions for both measurements. The movies were not processed to avoid changes of the intensity.

2.2.7. Total internal reflection microscopy (TIRF- microscopy)

Components

The TIRF microscope was purchased from TILL photonics. It was placed on a vibration-free optical table.

- iMIC

  The iMIC microscope has a motorized filter change and a stepper motor in z- direction with 2 µm resolution included, supported by a piezo z- drive with a resolution of 50 nm for all objectives. A plan- apochromat Olympus 100x/ NA 1.45 Plan APO TIRFM objective was used. An immersion oil with n= 1.516 was put onto the objective. The iMIC was controlled by an external unit.

- Scanhead

The galvanometer- driven scan head regulated by a computer- controlled mode switch element directs the laser beam into the microscope and determines the TIRF angles.

- Filters- only GFP is missing!!!!!!!!!

A dual excitation filter set with specification of 488/10 and 560/20 was used. The dual emission filter had the following specifications: 525/50 (GFP filter) and 610/75 (rhodamine filter)

- Laser

The Coherent Sapphire DPSS laser with 75 mW at 488 nm was used to excite GFP and the Cobolt Jive DPSS laser with 75 mW at 561 nm was used to excite RFP (mKate2).

- Camera

The images were recorded with an Andor IXON+ DU897ECS camera with a chip of 512x512 pixels. In front of the camera a 2x magnifying lens was placed. The camera had a quantum efficiency of 92 % at 500 nm and sampling rates of 10, 5, 3 and 1 MHz. For recording the electron multiplying (EM) gain of the camera was set up to -300 V.

- Software

Images were acquired using 'Live Acquisition Software'

Microscopy

- Coverslip cleaning

The coverslips were put into 1 M NaOH and shook on the UNITWIST 3D shaker for 4 – 7 h. Then they were washed in ddH_2O twice for 5 min. Before the coverslips were stored in absolute ethanol the previous process was repeated.

- Sample preparation

A colony was picked with a sterile pipette tip and inoculated in 1 mL SCD-all overnight at 30 °C. Two hours before microscopy 100 µL of the overnight culture was diluted with 1 mL SCD-all and incubated again until the cultures had an OD between 0.4 and 0.8.

A coverslip was taken out of the absolute ethanol and dried with pressure air. Afterwards 4.5 µL ConA (2 mg/mL) was put onto the coverslip and distributed on the surface, which was then dried

with compressed air. On the prepared coverslip 4.5 µL of the cell culture was added. Finally the coverslip was put onto a slide. One sample was examined for maximal 45 min.

2.2.8. Evaluation of microscopy data

The movies recorded with the TIRF- Microscope were evaluated with the program ImageJ developed by Wayne Rasband. Details of data evaluation can be seen at the chapter results.

3. Results

3.1. Sso1- mKate2 plasmid

The aim of this experiment was to construct a plasmid for tagging the t-SNARE Sso1 with the RFP mKate2. Because the t-SNARE Sso1 is a tailed anchored protein with a different biosynthesis pathway, the protein has to be tagged at the N-terminal end. Therefore a plasmid was constructed in which the mKate2 fluorophore was placed between the sequence of the promoter of the Sso1 Protein and the gene sequence of the gene. The method of tagging the gene exogenous was chosen because it is a fast and easy way for protein tagging. Moreover the danger producing nonviable strains was avoided as it can happen when the strain would be tagged endogenous hence a functional gene sequence is still available in the genome.

3.1.1. Cloning of genes into pJET1.2 plasmid

Genomic DNA of BY4741 was used as a source to amplify gene and promoter of Sso1 and mKate2 was amplified from a plasmid. New restricticion sites had to be added for the later ligation. To amplify the sequences the PCR product of each DNA sequence was cloned into a pJet1.2 plasmid to transform them into *E.coli* cells. The plasmids of some growing cultures were isolated and pre-checked with an agarose gel electrophoresis after the digestion with BglII. The expected length of the fragments was determined with the software ApE.

Table 16: Expected sequence lengths of the DNA fragments after PCR

Gene	Sequence length [bp]
pSso1	335
Sso1	517; 370 (the gene has itself a BglII restriction site)
mKate2	710

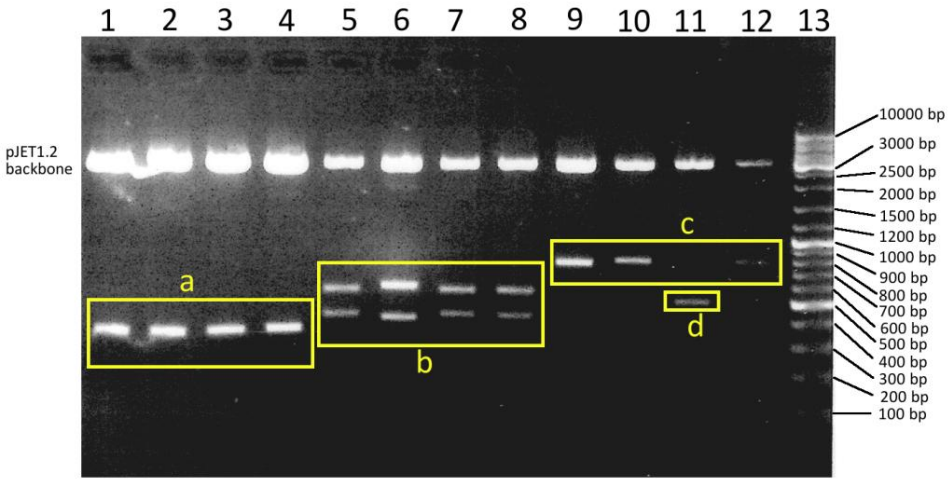

Figure 9: Test digestion of pJET1.2 plasmids ligated with pSso1, Sso1 and mKate2 on a 1% agarose gel

Lane 1: Plasmid F1 (pJet1.2+pSso1); Lane 2: Plasmid F2 (pJet1.2+pSso1); Lane 3: Plasmid F3 (pJet1.2+pSso1); Lane 4: Plasmid F4 (pJet1.2+pSso1); Lane 5: Plasmid F5 (pJet1.2+Sso1); Lane 6: Plasmid F6 (pJet1.2+Sso1); Lane 7: F1 (pJet1.2+Sso1); Lane 8: Plasmid F8 (pJet1.2+Sso1); Lane 9: F9 (pJet1.2+mKate2); Lane 10: F10 (pJet1.2+mKate2); Lane 11: F11 (pJet1.2+mKate2); Lane 12: F12 (pJet1.2+mKate2); Lane 13: 5 µL GeneRuler™ DNA ladder Mix

In every lane the fragment of the pJET1.2 backbone can be seen a little above the 3000 bp fragment of the marker. This indicates the proper function of the reaction mixture for the control digestion. In lane one to four fragments (a) with an approximately length of 300 bp can be detected. The lengths agree with the expected length of pSso1. Thus these plasmids include the right inserts. In every lane from 5 to 8 two bands (b) can be seen with the approximately lengths of 400 bp and 500 bp which corresponded to the expected lengths of the fragments. According to gel picture in Figure 1, the plasmids carry the right insert. A fragment of 700 bp length (c) is detected in lane 9, 10 and 12. This is consistent with the calculated length of mKate2. Only in lane 11 a fragment (d) with a length of 500 bp is observed which differed from the calculations. This result suggests that only the plasmids in lane 9, 10 and 12 have the right inserts. A reason for the short fragment in lane 11 could be an abandoned elongation during the PCR or a double strand break which took place in the previous processes. If the plasmids are inserted in the right direction and to exclude any changes of the sequence compared to the origin ones, the plasmids which seem to have the right inserts were sequenced. After the evaluation of the sequencing result it is clarified that the inserts of plasmid F1, F7 and F9 had also the right sequence and direction.

3.1.2. Control of the final plasmid

After the verification of the pJET1.2 plasmids they were amplified in *E.coli*. Then the inserts were isolated and purified. With these DNA solutions ligation was performed to ligate the three inserts and

the pTL58 backbone. The ligated plasmids were transformed in E.coli, following, plasmid isolation of grown *E.coli* cultures was conducted. The isolated plasmids were digested to check on an agarose gel if the ligation had worked.

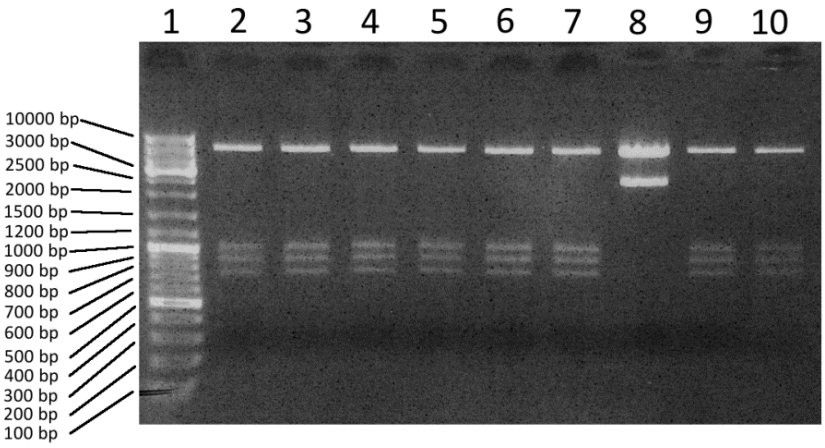

Figure 10: Control digestion of the plasmid pTL58-pSso1-mKate2-Sso1 on a 1% agarose gel

Lane 1: 5 µL GeneRuler™ DNA ladder Mix; Lane 2: F13 plasmid (pTL58-pSso1-mKate2-Sso1) ; Lane 3: F14 plasmid (pTL58-pSso1-mKate2-Sso1) ; Lane 4: F15 plasmid (pTL58-pSso1-mKate2-Sso1) ; Lane 5: F16 plasmid (pTL58-pSso1-mKate2-Sso1) ; Lane 6: F17 plasmid (pTL58-pSso1-mKate2-Sso1) ; Lane 7: F18 plasmid (pTL58-pSso1-mKate2-Sso1) ; Lane 8: F19 plasmid (pTL58-pSso1-mKate2-Sso1) ; Lane 9: F20 plasmid (pTL58-pSso1-mKate2-Sso1) ; Lane 21: F21 plasmid (pTL58-pSso1-mKate2-Sso1)

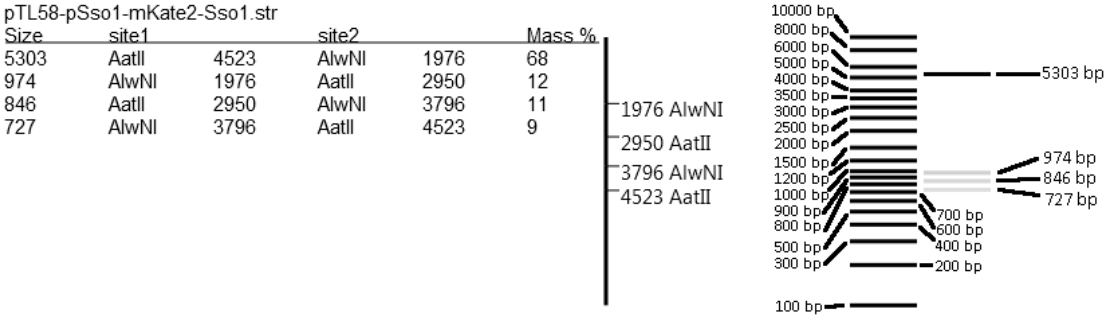

Figure 11: Theoretical digestion of pTL58-pSso1-mKate2-Sso1

Figure 3 illustrates the theoretical control digestion of the pTL58-pSso1-mKate2-Sso1 plasmid at the left. In the middle the figure shows the location of the AlwNI and AatII restriction sites in the plasmid and on the right the expected separation of the fragments in the agarose gel is demonstrated. If the separation in the lanes of the agarose gel is compared to the theoretical separation, it is clear that all lanes show the expected length of the fragments except the lane 8 (Figure 2). The separation pattern in lane 8 displays a digested pTL58 plasmid without insert. The plasmid for tagging Sso1 with mKate2 N-terminal was created successfully. The plasmid map can be seen in Figure 4. Unfortunately the plasmid was not transformed because the project was handed over to another member of the lab.

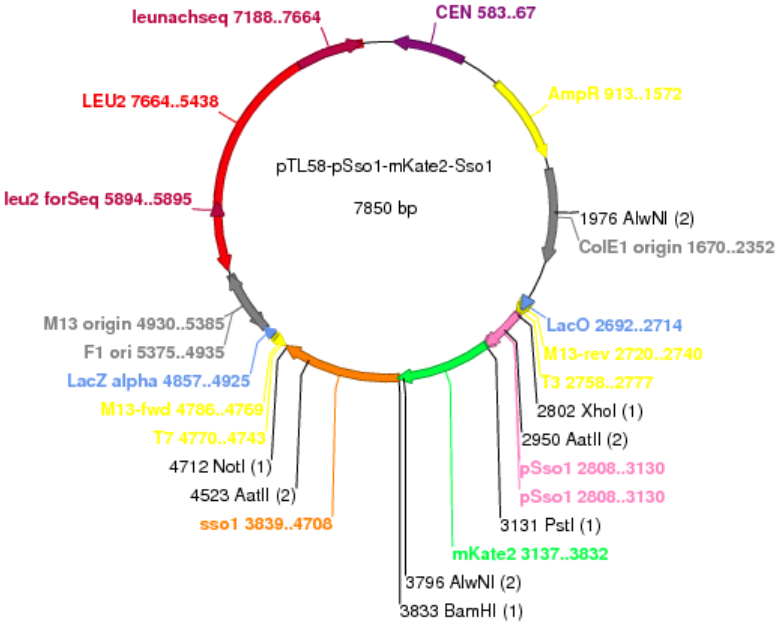

Figure 12: Plasmid map of pTL58-pSso1-mKate2-Sso1

3.2. Lifetime measurements

3.2.1. Data evaluation for lifetimes of single color strains

Determined lifetimes of each of the four subunits were plotted in a histogram and a single Gaussian was fitted to identify the lifetime of each subunit.

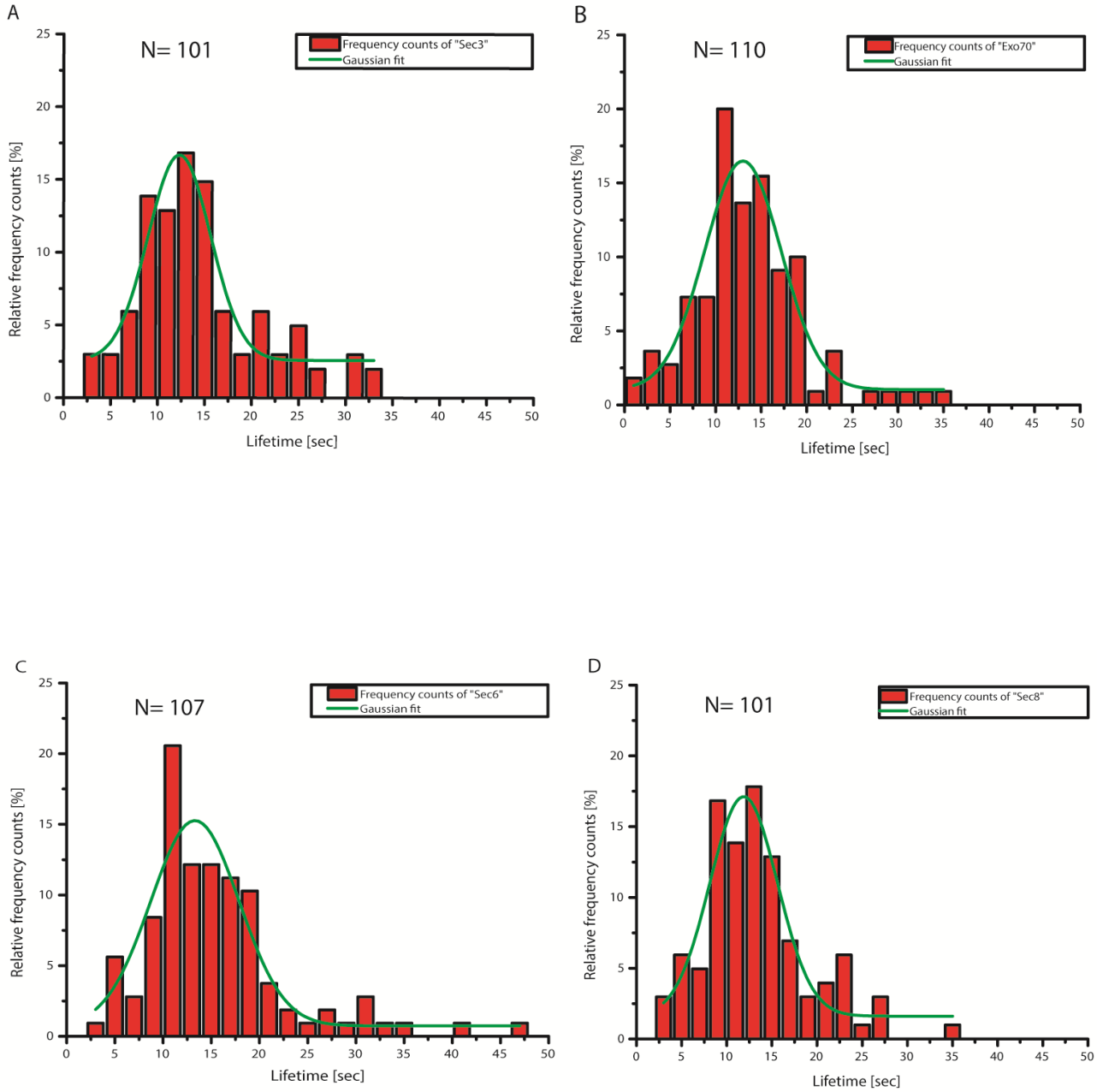

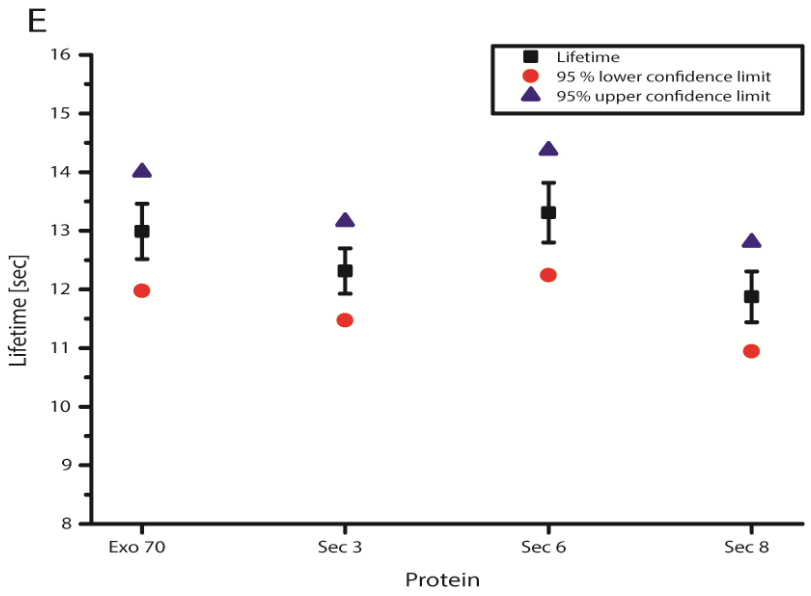

Figure 13: Histograms and summary of lifetime measurements of single color strains

A Histogram lifetime Sec3; B Histogram lifetime Exo70; C Histogram lifetime Sec6; D Histogram lifetime Sec8; E Summary of lifetime values

Table 17: Histogram bin size of lifetime measurements single color strains

Bin size	Bin center	Bin end
2	1+ (n · 2)	0 + (n · 2)

Table 18: Statistical values and parameters of the fit single color strains

Figure 6	Fitted model	Reduced Chi-Square	p-value	Adjusted R-Square	x_c	Standard error x_c
A (Sec3)	Gaussian	3.981	0.046	0.857	12.313	0.387
B (Exo70)	Gaussian	5.614	0.018	0.841	12.989	0.473
C (Sec6)	Gaussian	5.279	0.022	0.824	13.039	0.510
D (Sec8)	Gaussian	5.289	0.021	0.848	11.873	0.431

Table 19: Values of the fit single color strains

Figure 6; E	Lifetime [sec]	Standard error lifetime [sec]	95% lower confidence limit	95% upper confidence limit
Sec3	12.313	0.387	11.469	13.157
Exo70	12.989	0.473	11.974	14.002
Sec6	13.039	0.510	12.241	14.376
Sec8	11.873	0.431	10.940	12.805

The reduced Chi- square value correlates with the significance level which is described by the p-value. A p-value under 0.05 is deemed to be significant. The R-square value is a dimension how good the fit is in explaining the variation of the data. The closer the R-square value is to 1 the better the predicted response values of the fit correlate to the response values. Thus with a higher R-square value a greater proportion of variance is accounted for by the fit. The R-square value rises with an increasing number of the degrees of freedom of the fit. Therefore the adjusted R-square value was used which is independent of the degrees of freedom.

All Gaussian fits of the histograms (Figure 8, A- D) have larger or equal reduced Chi- square values of 3.981 (Table 16). Thus all fits satisfy the significance criteria. Moreover the adjusted R-square values are between 0.824 and 0.857 (Table 16) which are good values and indicates that the fits match to the data.

The experiments revealed that all subunits have very similar lifetimes between 12 sec and 13 sec (Figure 8; E). In the limits of the standard error and of the confidence limits the lifetimes of the subunits are all the same.

3.3.Time- resolved colocalization

3.3.1. Exo70 Sec6 strains

In the following histograms the data of the strain was plotted in which Exo70 was tagged with GFP and Sec6 was tagged with mKate2.

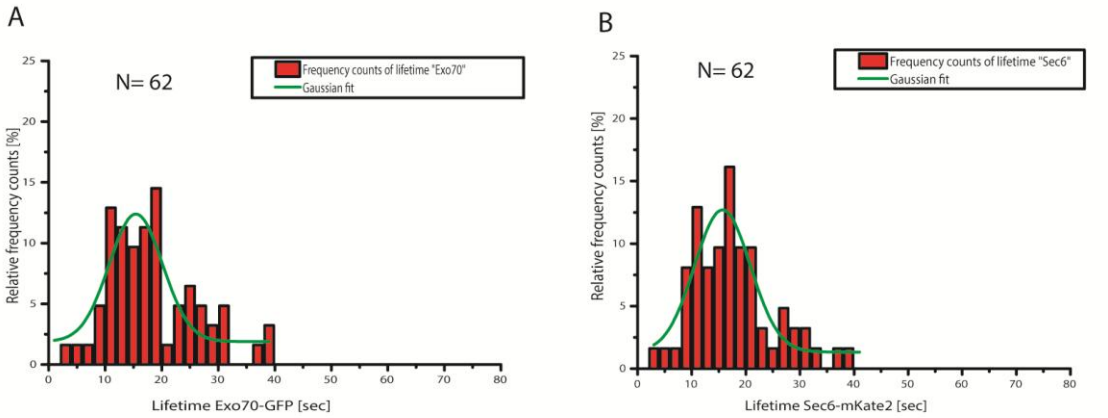

Figure 14: Lifetime histograms strain Exo70-GFP with Sec6-mKate2

A: Lifetime histogram of Exo70; B: Lifetime histogram of Sec6

Table 20: Histogram bin size of lifetime measurements strain Exo70-GFP with Sec6-mKate2

Bin size	Bin center	Bin end
2	1+ (n · 2)	0 + (n · 2)

Table 21: Statistical values and parameters of the fit strain Exo70-GFP with Sec6-mKate2

Figure 13	Fitted model	Reduced Chi-Square	p-value	Adjusted R-Square	x_c	Standard error x_c
A (Exo70-GFP)	Gaussian	7.902	0.005	0.620	15.421	0.874
B (Sec6-mKate2)	Gaussian	5.490	0.02	0.746	15.681	0.705

Table 22: Values of the fit strain Exo70-GFP with Sec6-mKate2

Figure 13	Lifetime [sec]	Standard error lifetime [sec]	95% lower confidence limit	95% upper confidence limit
Exo70-GFP	15.421	0.874	13.569	17.274
Sec6-mKate2	15.681	0.705	14.187	17.176

The Gaussian fits of the lifetime histograms (Figure 14) result in reduced Chi- square values of 7.902 (Exo70) and 5.490 (Sec6). Thus the fits are significant. The adjusted R-square (0.620 (Exo70) and 0.746 (Sec6)) values are too small.

The resulted lifetimes are about 15.421 sec for Exo70 and 15.681 sec for Sec6. Both proteins in this strain have very similar lifetime values. Notably, the measured lifetimes differ between single color strains and double color strains about 3 seconds. To examine the chronology of the colocolizing proteins histograms with lifetime differences, lifetime differences at appearance at disappearance were plotted.

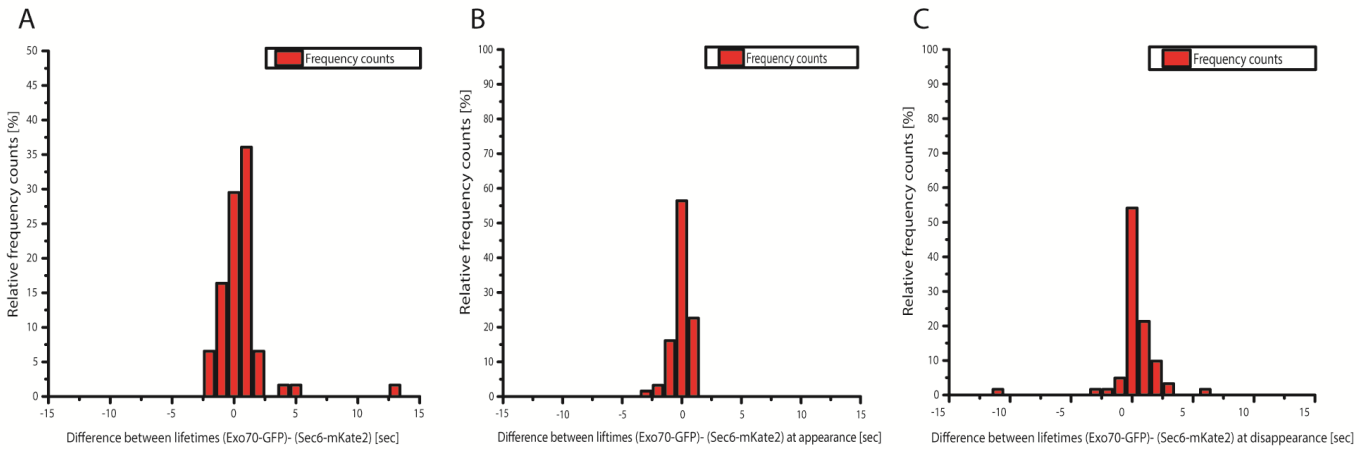

Figure 15: Lifetime difference histograms strain Exo70-GFP with Sec6-mKate2

A: Exo70 lifetime minus Sec6 lifetime histogram; B: Exo70 appearance minus Sec6 appearance; C: Sec6 disappearance minus Exo70 disappearance

Table 23: Histogram bin size of lifetime differences strain Exo70-GFP with Sec6-mKate2

Bin size	Bin center	Bin end
1	1± (n · 1)	0 ± (n · 0.5)

The histogram (Figure 15; A) which illustrates the differences between the lifetimes verify the same lifetimes of the proteins. The most frequency counts are in the region $-1.5 < \Delta t \leq 1.5$. The chronology was examined with histograms of appearance and disappearance (Figure 15; B, C). These histograms clarified that the proteins appear and disappear together hence the most frequency counts are between $-0.5 < \Delta \leq 0.5$.

The next step was to check whether the fluorophores itself have effects on the function of the proteins. Therefore movies of the strain with GFP tagged Sec6 and mKate2 tagged Exo70 were recorded.

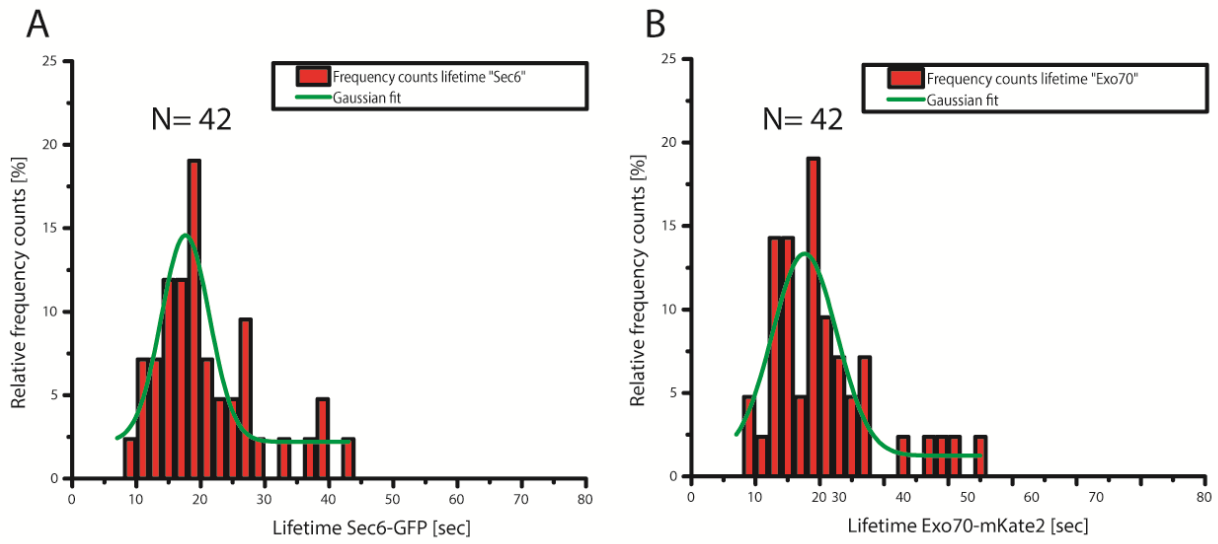

Figure 16 Lifetime histograms strain Sec6-GFP with Exo70-mKate2

A: Lifetime histogram of Sec6; B: Lifetime histogram of Exo70

Table 24: Histogram bin size of lifetime measurements strain Sec6-GFP with Exo70-mKate2

Bin size	Bin center	Bin end
2	1+ (n · 2)	0 + (n · 2)

Table 25: Statistical values and parameters of the fit strain Sec6-GFP with Exo70-mKate2

Figure 15	Fitted model	Reduced Chi-Square	p-value	Adjusted R-Square	x_c	Standard error x_c
A (Sec6-GFP)	Gaussian	12.42312	0.001	0.58279	17.63498	0.98186
B (Exo70-mKate2)	Gaussian	8.59696	0.003	0.66365	17.63755	0.68926

Table 26: Values of the fit strain Sec6-GFP with Exo70-mKate2

Figure 15	Lifetime [sec]	Standard error lifetime [sec]	95% lower confidence limit	95% upper confidence limit
Sec6-GFP	17.63498	0.98186	15.55354	19.71643
Exo70-mKate2	17.63755	0.68926	16.16843	19.10667

The fits of the histograms produces good reduced Chi-square values (12.423 and 8.597; Table 25) which indicate significance. The adjusted R-square values (0.583 and 0.664; Table 2) are too small hence the amount of data was small. The lifetimes of the proteins in this experiment were 17.635 (Sec6-GFP) and 17.638 (Exo70-mKate2) which are about 2 sec longer than the lifetimes of the Exo70-GFP with Sec6- mKate2 strain, but again the lifetimes of both proteins are very similar. The data

suggest that tagging Exo70 with mKate2 has a greater effect on function of the exocyst complex than tagging with GFP.

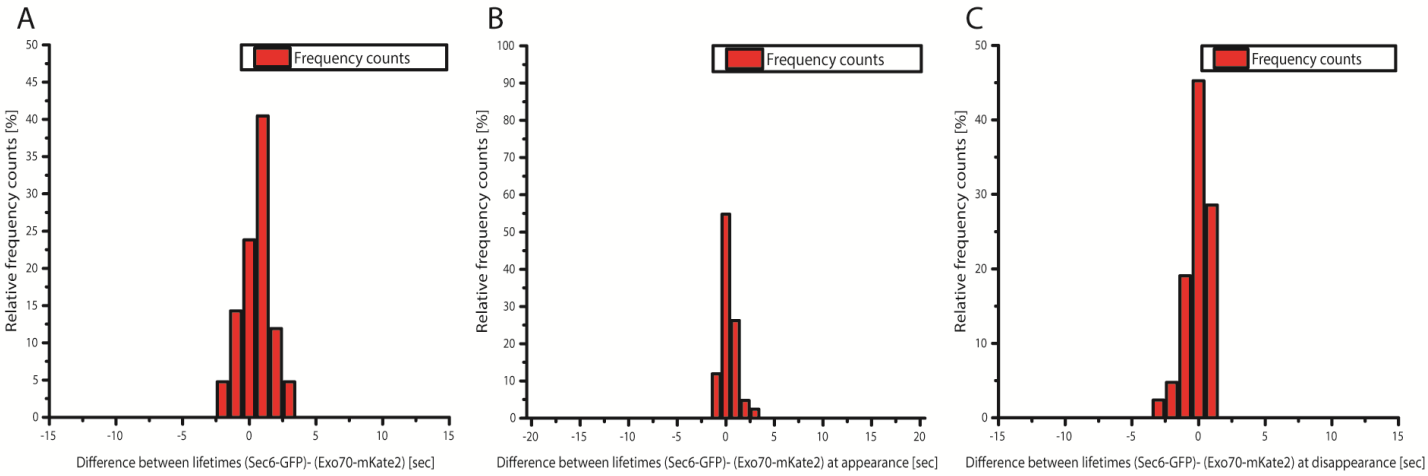

Figure 17: Lifetime difference histograms strain Sec6-GFP with Exo70-mKate2

A: Sec6 lifetime minus Exo70 lifetime histogram; B: Sec6 appearance minus Exo70 appearance; C: Exo70 disappearance minus Sec6 disappearance

Table 27: Histogram bin size of lifetime differences strain Sec6-GFP with Exo70-mKate2

Bin size	Bin center	Bin end
1	$0 \pm (n \cdot 1)$	$0 \pm (n \cdot 0.5)$

The most counts in all lifetime histograms resided in the range of $-1.5 < \Delta \leq 1.5$ for the lifetime differences and of $-0.5 < \Delta \leq 0.5$ for the appearance and disappearance, according to that the two proteins colocolize completely.

3.3.2. Sec3 Exo70 strain

In the next strain Sec3 was tagged with GFP and Exo70was tagged with mKate2.

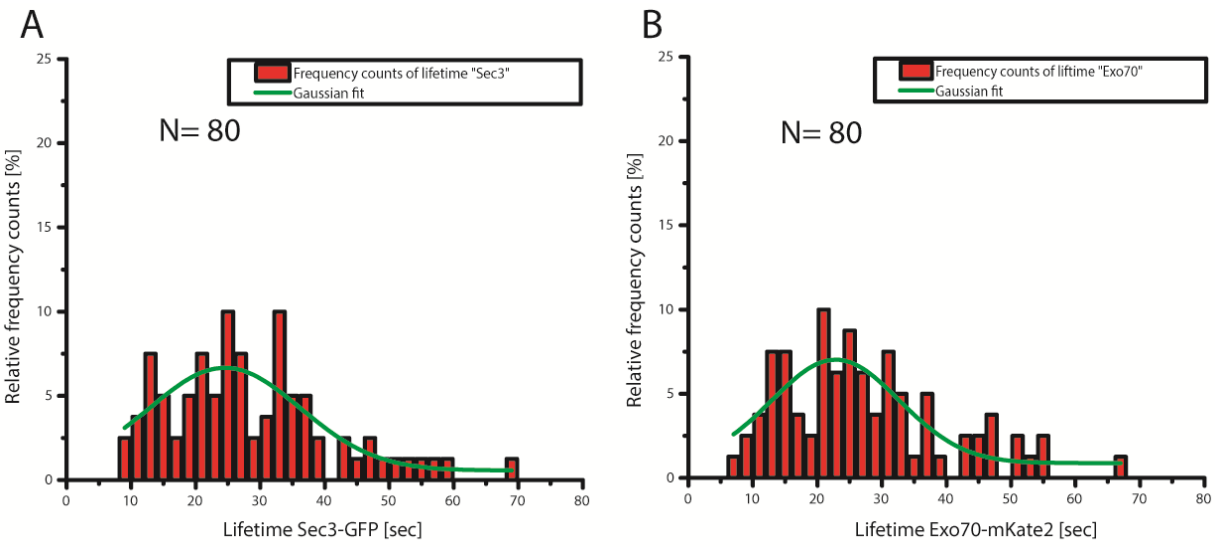

Figure 18 Lifetime histograms strain Sec3-GFP with Exo70-mKate2

A: Lifetime histogram of Sec3; B: Lifetime histogram of Exo70

Table 28: Histogram bin size of lifetime measurements strain Sec3-GFP with Exo70-mKate2

Bin size	Bin center	Bin end
2	1+ (n · 2)	0 + (n · 2)

Table 29: Statistical values and parameters of the fit strain Sec3-GFP with Exo70-mKate2

Figure 16	Fitted model	Reduced Chi-Square	p-value	Adjusted R-Square	x_c	Standard error x_c
A (Sec3-GFP)	Gaussian	3.51767	0.061	0.58193	22.81546	1.5027
B (Exo70-mKate2)	Gaussian	3.38682	0.065	0.59243	24.52343	1.72745

Table 30: Values of the fit strain Sec3-GFP with Exo70-mKate2

Figure 16	Lifetime [sec]	Standard error lifetime [sec]	95% lower confidence limit	95% upper confidence limit
Sec3-GFP	22.81546	1.5027	19.73219	25.89874
Exo70-mKate2	24.52343	1.72745	20.97899	28.06786

The reduced Chi-square values (3.518 and 3.387) are too low for significance and the adjusted R-square values (0.582 and 0.592) are also too small. Thus the resulted lifetimes of 23 sec (Sec3-GFP)

and 24 sec for (Exo70-mKate2) have less validity. In the lifetime histograms can be seen that the lifetimes have greater values and a broader spectrum than in previous measurements. This indicates that tagging of Sec3 with GFP and Exo70 with mKate2 has negative influences on the function of the proteins.

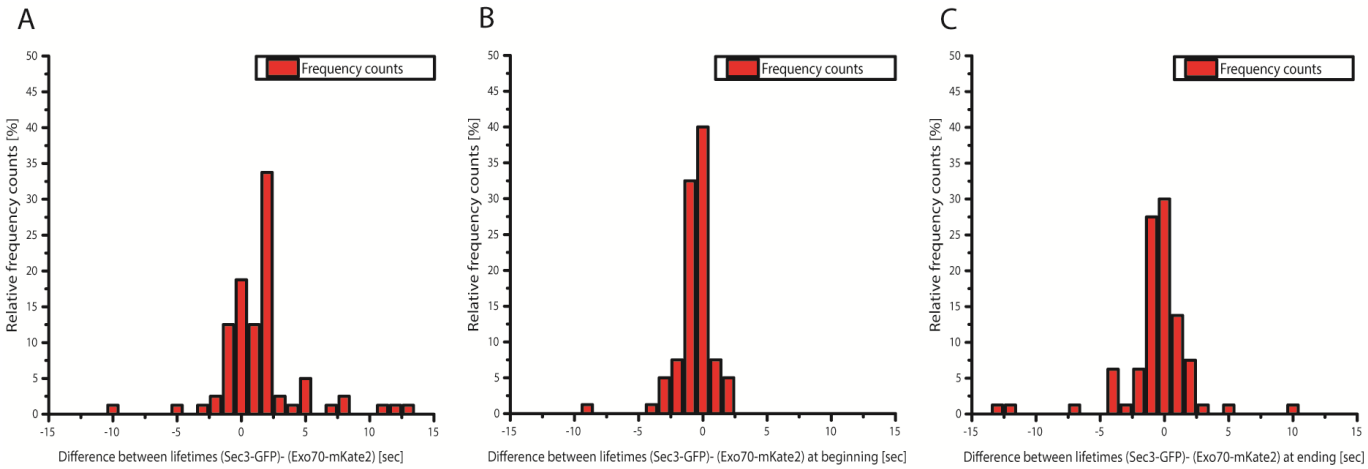

Figure 19: Lifetime difference histograms strain Sec3-GFP with Exo70-mKate2

A: Sec3 lifetime minus Exo70 lifetime histogram; B: Sec3 appearance minus Exo70 appearance; C: Sec3 disappearance minus Exo70 disappearance

Table 31: Histogram bin size of lifetime differences strain Sec3-GFP with Exo70-mKate2

Bin size	Bin center	Bin end
1	0± (n · 1)	0 ± (n · 0.5)

The histograms of the lifetime differences suggests a longer lifetime of Sec3 tagged with GFP because of the peak between $1.5 < \Delta t \leq 2.5$. But the histograms of appearance and disappearance show most of the patches a coming and leaving at the same time hence the peak of the frequency counts are between $-1.5 < \Delta t \leq 1.5$. So the peak in figure A originates because of little temporal variation at appearance and disappearance which produce the peak in the lifetime difference when they are added together. These variations could be explained with the temporal difference of the two different channels during recording or with the higher sensitivity for photobleaching of the fluorophore mKate2 and the different detection limit of mKate2. The histograms indicate the complete colocalization of Sec3 and Exo70.

In the next experiment the strain in which Exo70 was tagged with GFP and Sec3 was tagged with mKate2 was examined.

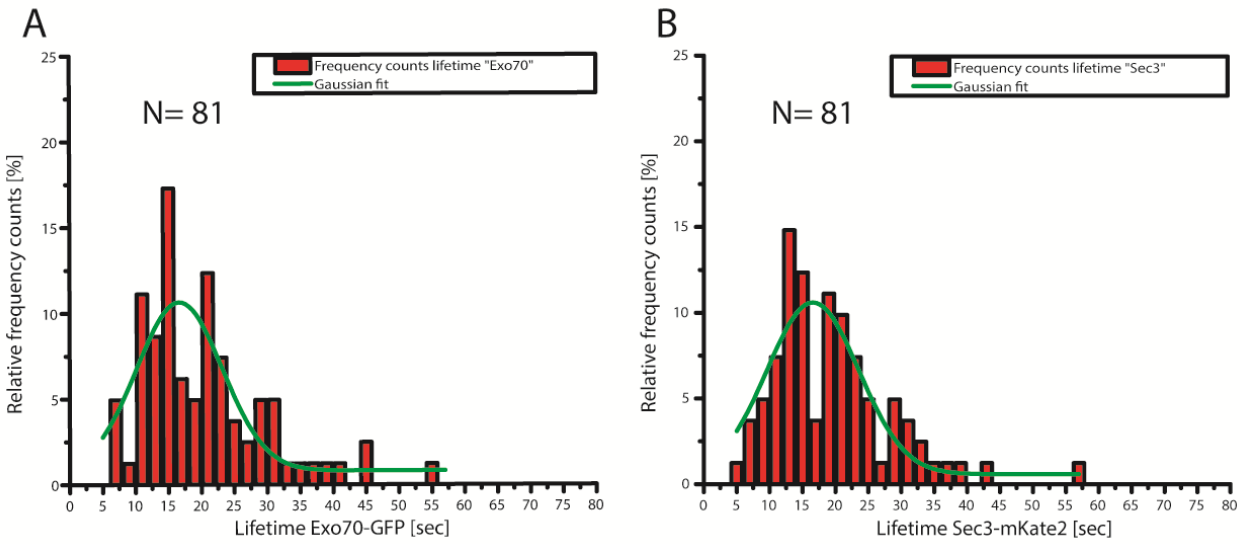

Figure 20: Lifetime histograms Exo70-GFP with Sec3-mKate2

A: Lifetime histogram of Exo70; B: Lifetime histogram of Sec3

Table 32: Histogram bin size of lifetime measurements strain Exo70-GFP with Sec3-mKate2

Bin size	Bin center	Bin end
2	1+ (n · 2)	0 + (n · 2)

Table 33: Statistical values and parameters of the fit strain Exo70-GFP with Sec3-mKate2

Figure 17	Fitted model	Reduced Chi-Square	p-value	Adjusted R-Square	x_c	Standard error x_c
A (Exo70-GFP)	Gaussian	4.82705	0.028	0.72914	16.5667	0.89364
B (Sec3-mKate2)	Gaussian	7.69919	0.006	0.60441	16.67718	1.09907

Table 34: Values of the fit strain Exo70-GFP with Sec3-mKate2

Figure 15	Lifetime [sec]	Standard error lifetime [sec]	95% lower confidence limit	95% upper confidence limit
Exo70-GFP	16.5667	0.89364	14.71806	18.41534
Sec3-mKate2	16.67718	1.09907	14.40358	18.95079

For fits of histograms the reduced Chi-square values (4.827 and 7.699; Table 32) indicate significance. The adjusted R-square values are too small (0.729 and 0.604). Both fits in the histograms result in a lifetime of 16.57 for Exo70-GFP and 16.68 for Sec3-mKate2. The lifetimes are in the same scale.

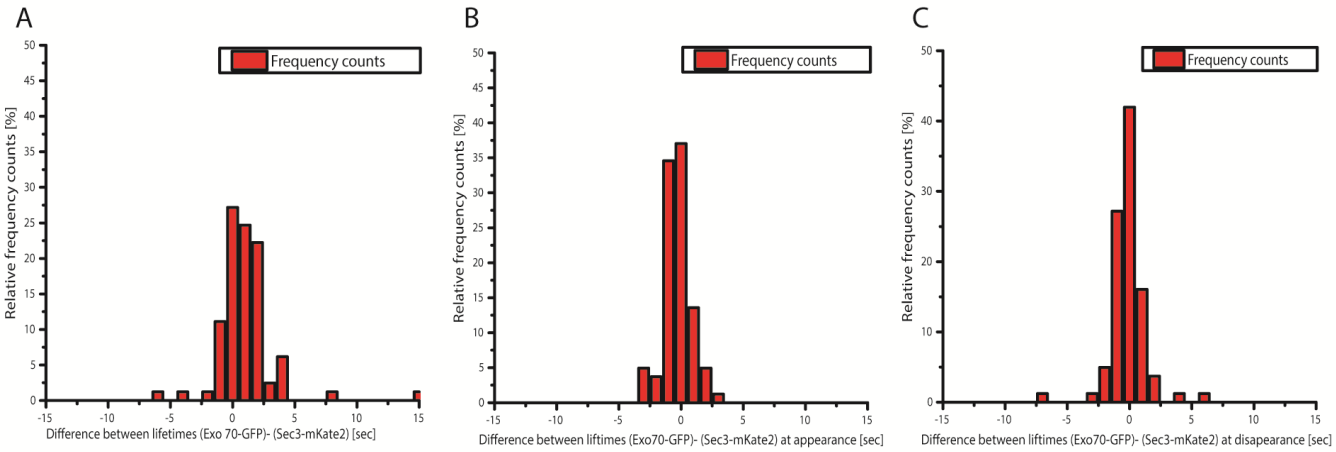

Figure 21: Lifetime difference histograms

A: Exo70 lifetime minus Sec3 lifetime histogram; B: Exo70 appearance minus Sec3 appearance; C: Sec3 disappearance minus Exo70 disappearance

Table 35: Histogram bin size of lifetime differences strain Exo70-GFP with Sec3-mKate2

Bin size	Bin center	Bin end
1	0± (n · 1)	0 ± (n · 0.5)

In all histograms (figure A, B and C) the most frequency counts are between $-1.5 < \Delta t \leq 1.5$. This indicates the proteins appear and disappear at the same time.

3.3.3. Sec6 Sec5 strain

In this experiment the strain in which Sec6 is tagged with GFP and Sec5 is tagged with mKate2 was measured.

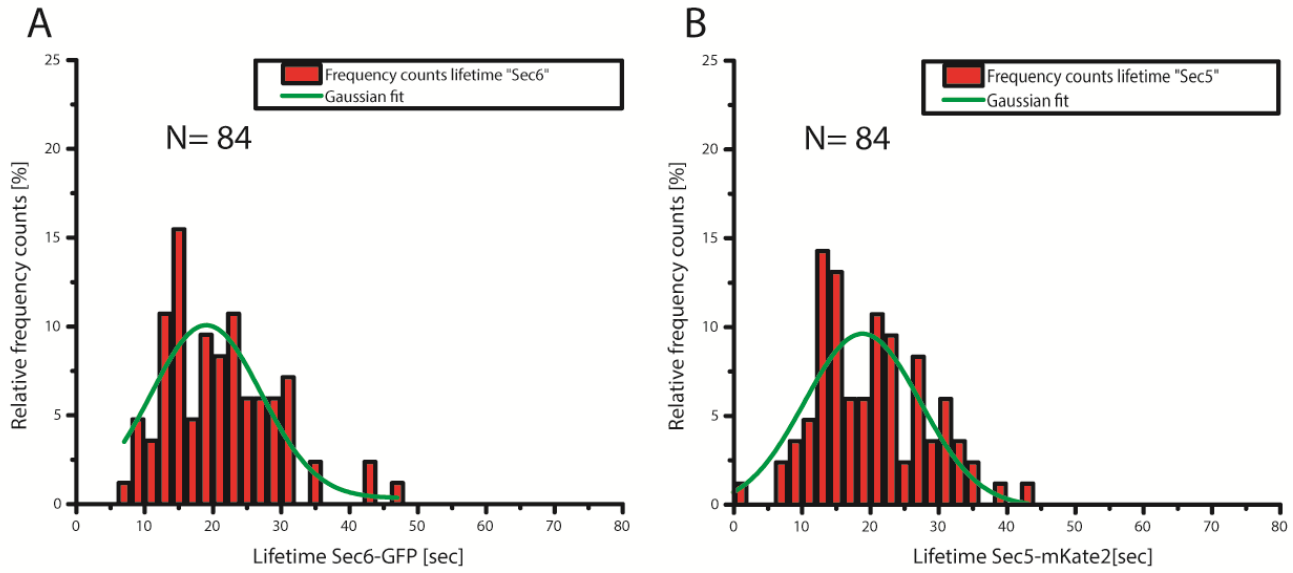

Figure 22: Lifetime histograms strain Sec6-GFP with Sec5-mKate2

A: Lifetime histogram of Sec6; B: Lifetime histogram of Sec5

Table 36: Histogram bin size of lifetime measurements strain Sec6-GFP with Sec5-mKate2

Bin size	Bin center	Bin end
2	1+ (n · 2)	0 + (n · 2)

Table 37: Statistical values and parameters of the fit strain Sec6-GFP with Sec5-mKate2

Figure 18	Fitted model	Reduced Chi-Square	p-value	Adjusted R-Square	x_c	Standard error x_c
A (Sec6-GFP)	Gaussian	7.90258	0.005	0.5699	18.82065	1.26656
B (Sec5-mKate2)	Gaussian	7.41722	0.006	0.61233	19.02619	1.25921

Table 38: Values of the fit strain Sec6-GFP with Sec5-mKate2

Figure 15	Lifetime [sec]	Standard error lifetime [sec]	95% lower confidence limit	95% upper confidence limit
Sec6-GFP	18.82065	1.26656	16.16971	21.4716
Sec5-mKate2	19.02619	1.25921	16.36948	21.6829

Both fits of the lifetime histograms have high Chi-square values (7.903 and 7.417). The adjusted R-square values (0.570 and 0.612) are too small. Both determined lifetimes of Sec6-GFP (18.82) and Sec5-mKate2 (19.02) have very similar values (Table 37).

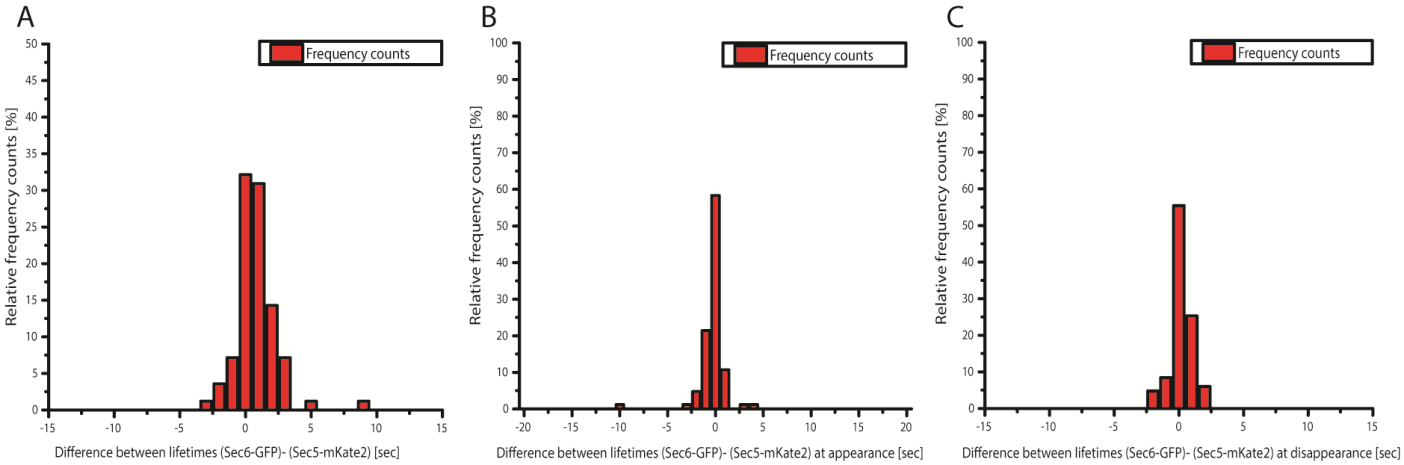

Figure 23: Lifetime difference histograms strain Sec6-GFP with Sec5-mKate2

A: Sec6 lifetime minus Sec5 lifetime histogram; B: Sec6 appearance minus Sec5 appearance; C: Sec5 disappearance minus Sec6 disappearance

Table 39: Histogram bin size of lifetime differences strain Sec6-GFP with Sec5-mKate2

Bin size	Bin center	Bin end
1	0± (n · 1)	0 ± (n · 0.5)

The histogram of the lifetime difference confirm the same lifetimes of the proteins (Figure 22; A). Moreover the histograms of appearance and disappearance reveal that the proteins appear and disappear together (Figure 22; B, C). Thus the two proteins colocalize completely.

3.3.4. Summary of the double color results

Table 40: Summary lifetimes of double color strains

Lifetimes	GFP lifetime [sec]	mKate2 lifetime [sec]
Sec3-GFP Exo70-mKate2	23	24
Exo70-GFP Sec3-mKate2	16.5	16.5
Sec6-GFP Exo70-mKate2	17.5	17.5
Exo70-GFP Sec6-mKate2	15.5	15.5
Sec6-GFP Sec5-mKate2	19	19

The evaluation showed the lifetimes of both proteins tagged in the double color strains are very similar. In every measured double color strain the subunits of the exocyst complex have longer lifetimes compared to the lifetime measurements with a single GFP tag. The lifetimes are shifted from 12- 13 sec to 16-18 sec. Furthermore, same proteins tagged with GFP showed different lifetimes than with a mKate2 tag. Therefore the different fluorophores constrain the function of the proteins in different ways. The strain Sec3-GFP with Exo70-mKate2 showed 6 -8 sec prolonged lifetimes compared to the strain Exo70-GFP with Sec3-mKate2. Also the strain Sec6-GFP with Exo70-mKate2 revealed prolonged lifetimes of about 3 sec compared to Exo70-GFP with Sec6-mKate2. These observations indicate that the mKate2 tag constrains the function of Exo70 more than a GFP tag does.

Another common characteristic which can be seen in the lifetime difference histogram are the many frequency counts in the range of $0.5 < \Delta t \leq 2.5$ indicating a longer lifetime of the protein tagged with the GFP (Figure 14, 16, 18, 20, 22; A). This characteristic changes with strains, in which the same subunit were tagged with the other fluorophores, according to that it must be an effect generated by the characteristics of the fluorophores which limit the ability for recording. For example GFP is more photostable and emits more light than mKate2 hence the recording of GFP is more likely.

The fits of the histograms of the subunits lifetimes (Figure 14, 16, 18, 20, 22) have all too small adjusted R-square values. The reason is that the function of the exocyst complex with two tagged subunits is disturbed hence the release of the exocyst complex cannot be regulated precisely anymore. The irregular release of the exocyst complexes lead to a broader distribution of the lifetimes resulting in a small adjusted R-square values. But the high Chi-square values indicate that a mean value of the lifetimes of the disturbed exocyst complex exists which suggests that most of the time the same function of the subunit is disturbed. To increase the adjusted R-square value more patches should be measured. The colocalization results are not affected by the Chi-square values and the adjusted R- square values because the results of colocalization are independent of the fits.

Another thing which has to be reminded is that the red channel is recorded before the green channel. For example if one patch appears in the green channel the first time the red signal is not recorded until the next recording cycle. Therefore the red patch seems to be delayed, although the patches appear at the same time.

In some kymographs patches are present which stay the whole video at the same place. These patches indicate that exocyst complex is strongly disturbed in its function, which result in a frequent observation of such patches in one cell, or that the recorded patches were localized at an emerging bud where the patches stay over a longer period.

Another observation which indicates the complete colocalization of the subunits is the same observed movement. Some patches appear, stay at one place, move with a speed about 0.2 µm/s and finally stay again at the place until they disappear. The identical movement can be seen in the green and the red channel. Therefore the subunits must move together. A reason for the movement could be a non working fusion hence a new location for fusion has to be found.

3.4. Subunit counting of the exocyst complex

The number of subunits of the exocyst complex and the ratio between the subunits are interesting characteristics helping to describe and to understand the structure of the exocyst complex better. For this purpose Cse4 was used as an endogenous comparison standard. Strains were generated in which one subunit of the exocyst complex and Cse4 were tagged with GFP.

The corrected integrated densities of the Cse4 and the subunits of the exocyst complex were blotted in histograms. The data for the Cse4 histogram were obtained from three different strains (Sec3-GFP Cse4-GFP, Sec5-GFP Cse4-GFP and Sec6-GFP Cse4-GFP).

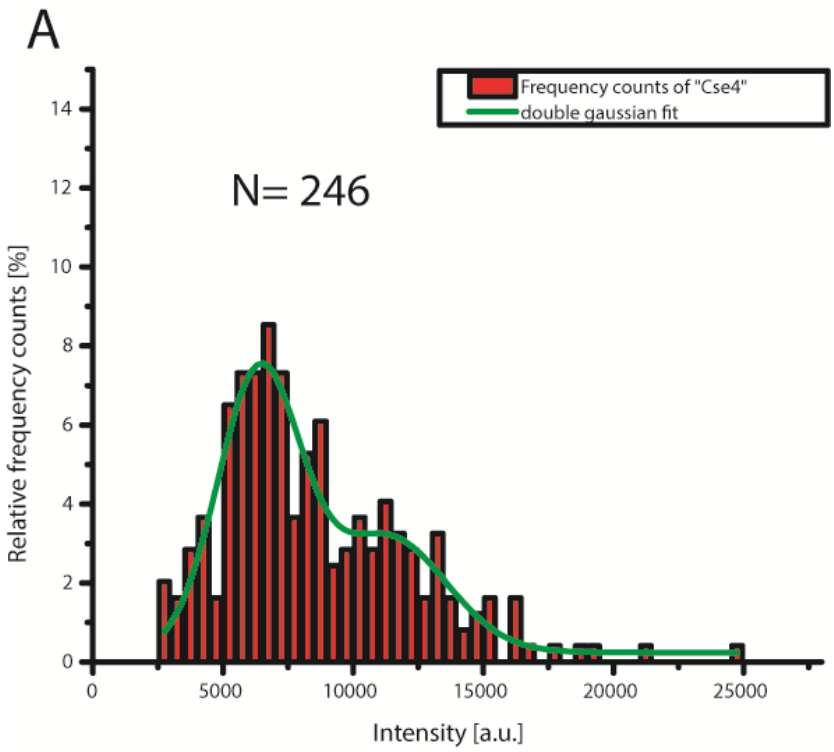

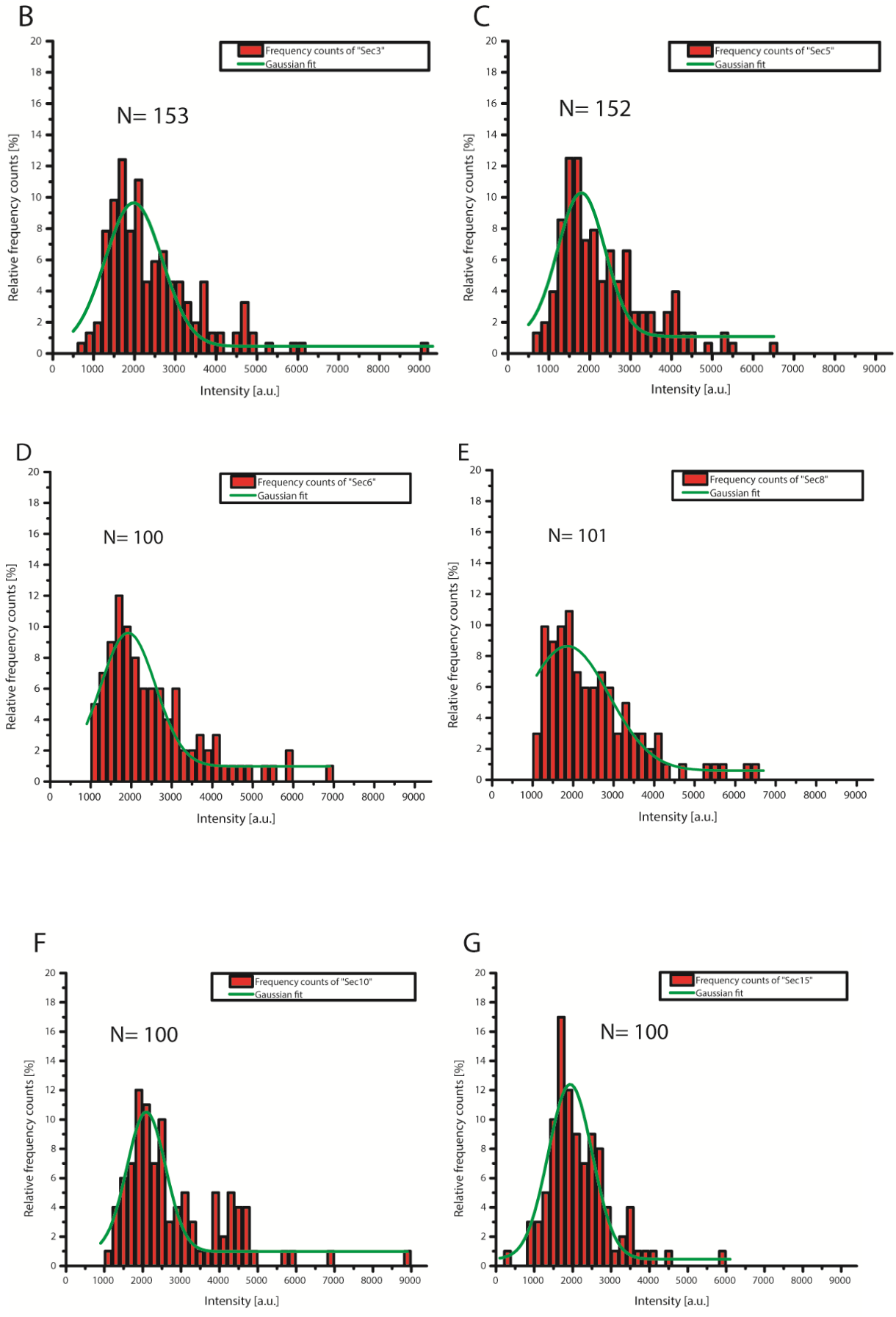
B
Frequency counts of "Sec3"
Gaussian fit
N= 153
Relative frequency counts [%]
Intensity [a.u.]
C
Frequency counts of "Sec5"
Gaussian fit
N= 152
Relative frequency counts [%]
Intensity [a.u.]
D
Frequency counts of "Sec6"
Gaussian fit
N= 100
Relative frequency counts [%]
Intensity [a.u.]
E
Frequency counts of "Sec8"
Gaussian fit
N= 101
Relative frequency counts [%]
Intensity [a.u.]
F
Frequency counts of "Sec10"
Gaussian fit
N= 100
Relative frequency counts [%]
Intensity [a.u.]
G
Frequency counts of "Sec15"
Gaussian fit
N= 100
Relative frequency counts [%]
Intensity [a.u.]

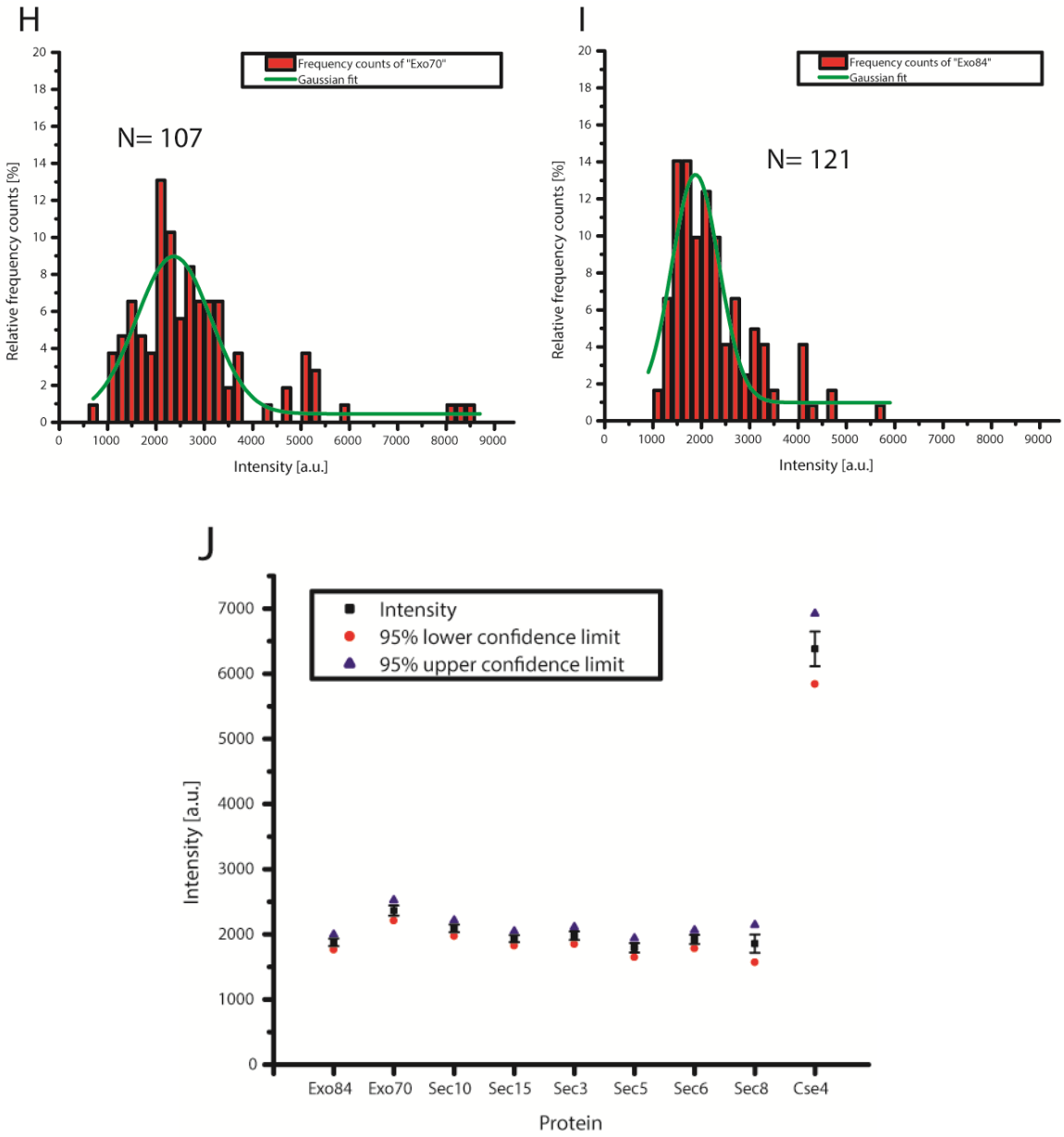

Figure 24: Histograms of measured intensities for quantification

A: Histogram of Cse4 intensities; B: Histogram of Sec3 intensities; C: Histogram of Sec5 intensities; D: Histogram of Sec6 intensities; E: Histogram of Sec8 intensities; F: Histogram of Sec10 intensities; G: Histogram of Sec15 intensities; H: Histogram of Exo70 intensities; I: Histogram of Exo84 intensities; J: Summary of the intensities obtained from the fits

Table 41: Histogram bin size of intensities measurements subunit counting

Figure 24	Bin size	Bin center	Bin end
A	500	2750+ (n · 500)	300 + (n · 2)
B- I	200	100+ (n· 200)	200 + (n· 200)

Table 42: Statistical values and parameters of the fit subunit counting

Figure 24	Fitted model	Reduced Chi-Square	p-value	Adjusted R-Square	x_c	Standard error x_c
A (Cse4)	Double Gaussian	0.791	0.374	0.865	6381 /1.Peak	266
					11297/ 2.Peak	860
B (Sec3)	Gaussian	2.258	0.133	0.791	1979	65
C (Sec5)	Gaussian	3.224	0.073	0.745	1793	70
D (Sec6)	Gaussian	2.085	0.149	0.817	1922	68
E (Sec8)	Gaussian	1.862	0.172	0.842	1855	13
F (Sec10)	Gaussian	2.858	0.091	0.730	2092	59
G (Sec15)	Gaussian	3.132	0.077	0.836	1934	53
H (Exo70)	Gaussian	2.535	0.125	0.762	2365	78
I (Exo84)	Gaussian	4.370	0.037	0.797	1877	56

Table 43: Values of the fit subunits counting

Figure 24	Intensity [sec]	Standard error intensity [sec]	95% lower confidence limit	95% upper confidence limit
Cse4/ 1.Peak 2.Peak	6381 11297	266 860	5841 9555	6921 13038
Sec3	1979	65	1848	2111
Sec5	1793	70	1648	1938
Sec6	1922	68	1782	2063
Sec8	1855	13	1570	2141
Sec10	2092	59	1971	2213
Sec15	1934	53	1825	2044
Exo70	2365	78	2207	2524
Exo84	1877	56	1760	1995

The Cse4 histogram (Figure 24, A) was fitted with a double Gaussian curve because this fit resulted in the best adjusted R-square value. Therefore the data suggest two peaks, one with intensity of 6381 and another one with an intensity value of 11297. Biological it makes sense because it is possible to measure the single chromosome set and the double replicated chromosome set. Thus you would expect one peak at certain intensity and a second one two times the intensity of the first peak. Unfortunately the reduced Chi-square is very low subsequently the fit is not significant. However the determined values can be used as an approximate indication for further comparisons.

All other histograms (Figure 24, B- I) were fitted with single Gaussian curves because only single vesicles were expected. The fits match well with the data as the adjusted R-square values show (Table 41). Only one fit of Exo84 has a Chi-square value which indicates significance. The Chi-square values of the other fits are too small for significance, but if one have a look at the intensities of each subunit determined by the fits it can be seen that the intensities of each subunit are in the same range of about 2000 (Figure 24, J). Hence it is likely that the obtained intensities correlate to the real

amount of subunits bound to the vesicles, although the Chi-square values do not indicate significance. Out of these data it was concluded that all subunits must occur in the identical stoichiometry. Thus one protein of every subunit is needed to form the exocyst complex.

Mean value of subunit intensities: 1977 a.u.

Table 44: Stoichiometry of the subunits

Subunit	Measured intensity	Ratio (measured intensity: mean value)
Sec3	1979	1,00
Sec5	1793	0,91
Sec6	1922	0,97
Sec8	1855	0,94
Sec10	2092	1,06
Sec15	1934	0,98
Exo70	2365	1,20
Exo84	1877	0,95

One chromosome set contains 80 to 128 copies of Cse4 [15, 16]. The ratio between the amount of the Cse4 copies and the determined intensity can be used for calibration. With results of the experiments the quantity of every subunit which is bound to one vesicle can be calculated roughly.

Table 45: Amount of one subunit connected to one vesicle

Subunit	Amount of the subunit depending on 80 copies of Cse4	Amount of the subunit depending on 128 copies of Cse4
Sec3	25 ± 1	40 ± 1
Sec5	22 ± 1	36 ± 1
Sec6	24 ± 1	39 ± 1
Sec8	23 ± 0	37 ± 0
Sec10	26 ± 1	42 ± 1
Sec15	24 ± 1	39 ± 1
Exo70	30 ± 1	47 ±2
Exo84	24 ± 1	38 ± 1

Finally the quantification experiment revealed that around 24 – 40 exocyst complexes are bound to one vesicle.

4. Discussion

Table 46: Summary of results

Subunits	Lifetime single color GFP [sec]	Lifetime double color GFP [sec]/ other tagged subunit	Lifetime double color mKate2 [sec]/ other tagged subunit	Subunits colocalizes with	Counted number of subunits relating to Cse4 copies 80	128
Sec3	12.3	22.8/Exo70	16.8/Exo70	Exo70	25 ± 1	40 ± 1
Sec5	-	-	19.0/Sec6	Sec6	22 ± 1	36 ± 1
Sec6	13.0	17.6/ Exo70; 18.8/Sec5	15.7/Exo70	Sec6; Exo70	24 ± 1	39 ± 1
Sec8	11.9	-	-	-	23 ± 0	37 ± 0
Sec10	-	-	-	-	26 ± 1	42 ± 1
Sec15	-	-	-	-	24 ± 1	39 ± 1
Exo70	13.0	15.4/Sec6; 16.6/Exo70	17.6/Sec6; 24.5/Sec3	Sec3; Sec6	30 ± 1	47 ±2
Exo84	-	-	-		24 ± 1	38 ± 1

The aim of the bachelor thesis was to monitor the dynamic behavior of the exocyst subunits. Measurements of strains in which single exocyst subunits were tagged with GFP revealed the same lifetimes 12- 13 sec for the subunits Sec3, Sec6, Sec8 and Exo70. The experiments with double color strains with one subunit tagged with mKate2 and another subunit tagged with GFP revealed the complete colocalization of Sec3 with Exo70, Sec6 with Exo70, and Sec6 with Sec5.

The lifetime measurements of double color strains, which resulted in lifetimes about 15.5 sec- 22 sec, were longer than measured lifetimes of single GFP strains. Thus tethering of the vesicles seemed not to be affected, but the release of the exocyst subunits takes longer and seems not to be strictly regulated anymore which the small adjusted R-square values of the fits indicate. It is likely the fluorphores added to subunits disturb the interaction between the subunits and the regulatory proteins, because the number of fluorophores at the tagged exocyst complex causes steric obstacles. The vesicles could also be influenced in their ability to move because roughly 50 new molecules are bound to the vesicle tagged with two exocyst subunits. Probably this is the reason for the prolonged live cycle of yeast double color tagged strains.

The complete colocalization of the measured subunits and the same lifetime of the single color suggest the whole exocyst complex is delivered to the plasma membrane on the exocytic vesicles because the lifetimes are the same and the patches appear and disappear at the same time. The tagged subunits are moving with each other, which can be seen in the kymograph and supports our result. It was already reported Sec5, Sec6, Sec8, Sec10, Sec15, and Exo84 are delivered by the exocytotic vesicle to the plasma membrane bound to the exocyst complex [14], which is supported by our data. To verify this colocalization, experiments with all subunits should be conducted.

Sec3 was reported to function as a landmark because it is delivered to the plasma membrane before the vesicle arrives and the delivery is unaffected by disruptions of the secretory pathway, actin and cell cycle proteins [24]. Our data, which shows the common appearance and disappearance of Exo70, Sec3, Sec6 and Sec5, and immunofluorescence of endogenous Sec3 call this result into question [1].

Exo70 was described to be delivered to the plasma membrane on vesicles or to localize independently of vesicle traffic through direct association with Rho proteins [14]. In contrast the conclusion based on our data was Exo70 is delivered on the vesicle together with the other subunits to the plasma membrane.

In the double color videos about 15% single GFP patches and about 3% single mKate2 patches could be observed for all strains. Single GFP patches are observed more often because GFP is more photostable and brighter. Moreover, mKate2 needs more time to fold properly than GFP hence some observed patches could have carried imperfect folded mKate2 which could not be detected. If Exo70 and Sec3 would have the proposed characteristic of being localized at the plasma membrane before the vesicle with the other subunits arrives [14], one would expect more single GFP patches in the strains Exo70-GFP with Sec6-mKate2 and Sec6-GFP with Exo70-mKate2 or great variation in appearance and disappearance.

The quantification experiment revealed about 24 or 40 exocyst complexes each composed of all subunits with a stoichiometry of 1:1 are bound to one vesicle. At least for Sec3 and Exo70 one would expect different stoichiometry if they are located at the plasma membrane before the other subunits arrive because the localization independent from the vesicle delivery and therefore also independent of the other subunits would lead to another number. Therefore quantification experiment also suggests that all subunits arrive together at the plasma membrane bound to one vesicle. Further quantification for the other proteins that are part of exocytosis should be done for a better understanding of the mechanism.

The quantification experiment leads to some questions, why needs one vesicle more than one exocyst complex, how are they distributed on the vesicle and do all complexes communicate with regulatory proteins. The different exocyst complexes could serve as antenna of the vesicles to screen for a proper place for fusion. If fusion of a vesicle did not work the other exocyst complexes could be used to detect another place for fusion which can be observed in movements of vesicles at the plasma membrane. Actually it would be interesting if the number of exocyst complexes bound to a vesicle depends on the area of vesicle membrane to clarify the origin of the assembled exocyst complex. The broad distribution of the intensity histograms would support this hypothesis.

The location of the assembly could not be determined with the experiments but we concluded the subunits arrive together at the plasma membrane. Perhaps the exocyst is already bound to the trans golgi network membrane and is transferred to the vesicles by budding. Therefore the number of exocyst complexes bound to the vesicle membrane would correlate to the size of the vesicles.

5. List of tables

6. List of figures

7. References

1. Heider, M.R. and M. Munson, *Exorcising the exocyst complex.* Traffic, 2012. **13**(7): p. 898-907.
2. Orlando, K. and W. Guo, *Membrane organization and dynamics in cell polarity.* Cold Spring Harb Perspect Biol, 2009. **1**(5): p. a001321.
3. He, B. and W. Guo, *The exocyst complex in polarized exocytosis.* Curr Opin Cell Biol, 2009. **21**(4): p. 537-42.
4. Munson, M. and P. Novick, *The exocyst defrocked, a framework of rods revealed.* Nat Struct Mol Biol, 2006. **13**(7): p. 577-81.
5. Nicholson, K.L., et al., *Regulation of SNARE complex assembly by an N-terminal domain of the t-SNARE Sso1p.* Nat Struct Biol, 1998. **5**(9): p. 793-802.
6. TerBush, D.R., et al., *The Exocyst is a multiprotein complex required for exocytosis in Saccharomyces cerevisiae.* EMBO J, 1996. **15**(23): p. 6483-94.
7. Finger, F.P. and P. Novick, *Sec3p is involved in secretion and morphogenesis in Saccharomyces cerevisiae.* Mol Biol Cell, 1997. **8**(4): p. 647-62.
8. Liu, J. and W. Guo, *The exocyst complex in exocytosis and cell migration.* Protoplasma, 2012. **249**(3): p. 587-97.
9. He, B., et al., *Exo70 interacts with phospholipids and mediates the targeting of the exocyst to the plasma membrane.* EMBO J, 2007. **26**(18): p. 4053-65.
10. Alberts, B., *Molecular biology of the cell*. 5th ed. ed, ed. J. Wilson and T. Hunt2008, New York :: Garland Science.
11. Guo, W., et al., *The exocyst is an effector for Sec4p, targeting secretory vesicles to sites of exocytosis.* EMBO J, 1999. **18**(4): p. 1071-80.
12. Morgera, F., et al., *Regulation of exocytosis by the exocyst subunit Sec6 and the SM protein Sec1.* Mol Biol Cell, 2012. **23**(2): p. 337-46.
13. Grosshans, B.L. and P. Novick, *Identification and verification of Sro7p as an effector of the Sec4p Rab GTPase.* Methods Enzymol, 2008. **438**: p. 95-108.
14. Boyd, C., et al., *Vesicles carry most exocyst subunits to exocytic sites marked by the remaining two subunits, Sec3p and Exo70p.* J Cell Biol, 2004. **167**(5): p. 889-901.
15. Coffman, V.C., et al., *CENP-A exceeds microtubule attachment sites in centromere clusters of both budding and fission yeast.* J Cell Biol, 2011. **195**(4): p. 563-72.
16. Lawrimore, J., K.S. Bloom, and E.D. Salmon, *Point centromeres contain more than a single centromere-specific Cse4 (CENP-A) nucleosome.* J Cell Biol, 2011. **195**(4): p. 573-82.
17. Joglekar, A.P., et al., *Molecular architecture of a kinetochore-microtubule attachment site.* Nat Cell Biol, 2006. **8**(6): p. 581-5.
18. Axelrod, D., *Cell-substrate contacts illuminated by total internal reflection fluorescence.* J Cell Biol, 1981. **89**(1): p. 141-5.
19. Axelrod, D., *Total internal reflection fluorescence microscopy in cell biology.* Traffic, 2001. **2**(11): p. 764-74.
20. Janke, C., et al., *A versatile toolbox for PCR-based tagging of yeast genes: new fluorescent proteins, more markers and promoter substitution cassettes.* Yeast, 2004. **21**(11): p. 947-62.
21. Sternberg, S.R., *BIOMEDICAL IMAGE-PROCESSING.* Computer, 1983. **16**(1): p. 22-34.
22. Hoffman, D.B., et al., *Microtubule-dependent changes in assembly of microtubule motor proteins and mitotic spindle checkpoint proteins at PtK1 kinetochores.* Mol Biol Cell, 2001. **12**(7): p. 1995-2009.
23. Johnston, K., et al., *Vertebrate kinetochore protein architecture: protein copy number.* J Cell Biol, 2010. **189**(6): p. 937-43.
24. Finger, F.P., T.E. Hughes, and P. Novick, *Sec3p is a spatial landmark for polarized secretion in budding yeast.* Cell, 1998. **92**(4): p. 559-71.